AD_____

CONTRACT NUMBER DAMD17-95-C-5086

TITLE: Retrieval of Water Channels by Endocytosis in Renal Epithelia

PRINCIPAL INVESTIGATOR: Dr. Abdul J. Mia
Dr. Thomas Yorio

CONTRACTING ORGANIZATION: Jarvis Christian College
Hawkins, Texas 75765

REPORT DATE: July 1998

TYPE OF REPORT: Final

PREPARED FOR: U.S. Army Medical Research and Materiel Command
Fort Detrick, Maryland 21702-5012

REPORT DOCUMENTATION PAGE

Form Approved
OMB No. 0704-0188

1. AGENCY USE ONLY (Leave blank)	2. REPORT DATE	3. REPORT TYPE AND DATES COVERED
	July 1998	Final (5 Jun 95 - 4 Jun 98)

4. TITLE AND SUBTITLE
Retrieval of Water Channels by Endocytosis in Renal Epithelia

5. FUNDING NUMBERS
DAMD17-95-C-5086

6. AUTHOR(S)
Abdul J. Mia, Ph.D.
Thomas Yorio, Ph.D.

7. PERFORMING ORGANIZATION NAME(S) AND ADDRESS(ES)
Jarvis Christian College
Hawkins, TX 75765

8. PERFORMING ORGANIZATION REPORT NUMBER

9. SPONSORING/MONITORING AGENCY NAME(S) AND ADDRESS(ES)
Commander
U.S. Army Medical Research and Materiel Command
Fort Detrick, MD 21702-5012

10. SPONSORING/MONITORING AGENCY REPORT NUMBER

11. SUPPLEMENTARY NOTES

12a. DISTRIBUTION / AVAILABILITY STATEMENT
Approved for public release; distribution unlimited

12b. DISTRIBUTION CODE

13. ABSTRACT *(Maximum 200)*

Combat crew effectiveness is crucial during sustained and demanding military operations. In particular, how soldiers cope with conditions of excess heat and fluid deprivation will ultimately impact on their ability to carry out their stated objectives. If the kidney should become damaged or obstructed, the kidney will fail to respond to the hormone vasopressin, which is responsible for regulating water balance. Understanding the specific mechanisms involved in the regulation of water balance by the kidney will provide information needed to design preventive measures for dealing with potential adverse conditions that may result in water deprivation and decreased renal responsiveness to vasopressin. The present study is designed to determine the cellular mechanisms involved in reduced fluid reabsorption and membrane reorganization following the removal of the actions of ADH. It is proposed that following removal of hormone, proteinaceous water channels, located in the apical membrane, are internalized through a process of endocytosis, delivered to the cytosol as a consequence of changes in intracellular calcium concentrations, PKC enzyme activation and reorganization of the microfilament/microtubule system. These studies may lead to new drug or non-drug treatment regimes that could be used to enhance the kidney's responsiveness to vasopressin or to maintain the level of water reabsorptive capacity of soldiers facing harsh environmental conditions of prolonged exposure to dehydration and water deprivation or impaired renal function from injury. Such preventive measures will be essential for maintaining the performance and combat effectiveness of our military forces.

14. SUBJECT TERMS
Water flow; ADH (vasopressin); Endocytosis; Water Channels; Channel Retrieval; Membrane Retrieval

15. NUMBER OF PAGES
64

16. PRICE CODE

17. SECURITY CLASSIFICATION OF REPORT	18. SECURITY CLASSIFICATION OF THIS PAGE	19. SECURITY CLASSIFICATION OF ABSTRACT	20. LIMITATION OF ABSTRACT
Unclassified	Unclassified	Unclassified	Unlimited

FOREWORD

Opinions, interpretations, conclusions and recommendations are those of the author and are not necessarily endorsed by the US Army.

X
____ Where copyrighted material is quoted, permission has been obtained to use such material.

X ___ Where material from documents designated for limited distribution is quoted, permission has been obtained to use the material.

X ___ Citations of commercial organizations and trade names in this report do not constitute an official Department of Army endorsement or approval of the products or services of these organizations.

X ___ In conducting research using animals, the investigator(s) adhered to the "Guide for the Care and Use of Laboratory Animals," prepared by the Committee on Care and Use of Laboratory Animals of the Institute of Laboratory Resources, National Research Council (NIH Publication No. 86-23, Revised 1985).

N/A For the protection of human subjects, the investigator(s) adhered to policies of applicable Federal Law 45 CFR 46.

N/A In conducting research utilizing recombinant DNA technology, the investigator(s) adhered to current guidelines promulgated by the National Institutes of Health.

N/A In the conduct of research utilizing recombinant DNA, the investigator(s) adhered to the NIH Guidelines for Research Involving Recombinant DNA Molecules.

N/A In the conduct of research involving hazardous organisms, the investigator(s) adhered to the CDC-NIH Guide for Biosafety in Microbiological and Biomedical Laboratories.

A. J. Mia 7/6/98

PI - Signature Date

TABLE OF CONTENTS

ABSTRACT

Pretreatment and removal of vasopressin (ADH) in toad urinary bladder renal model tissues induces endocytosis at 25°C. This study was carried out to determine if apical membrane remodeling, as well as transepithelial water flow, can be affected by lowering the temperature to 15°C. Control toad urinary bladders in the presence of an osmotic gradient at either 25° or 15°C when visualized by scanning electron microscopy (SEM) show a typical apical membrane surface with no apparent surface differences. ADH-treated tissues following 15 min stimulation at 25° or 15°C revealed a propagation of apical microvilli on their surface membranes. After 15 min following removal of ADH, bladder tissues at 25° or 15°C showed surface invaginations involving over 44% and 80% of granular cells, respectively. The rate of water flow in tissues at 15°C remained elevated compared to tissues held at 25°C. This was consistent with the observation that ADH-stimulated tissues following washout at 15°C still had marked apical membrane surface involvement. However, at 30 and 60 min post washout, ADH-stimulated tissues at 15°C recovered considerably, with a reduction in the number of shallow apical membrane invaginations involving fewer than 33% and 20% of granular cells respectively. This may indicate that the membrane undergoes continuous remodeling even in cold temperature conditions but at a different half-time. Control bladder tissues subjected to transmission electron microscopy (TEM) reveal a dense cytoplsmic profile with scattered distribution of secretory granules, rough ER cisternae, mitochondria and little or no vacuolation. In contrast, ADH-stimulated bladder tissues displayed a vacuolated cytoplasm, expanded rough ER cisternae and ruffled basolateral membranes. These observations suggest that the apical membrane undergoes considerable reorganization following cessation of hormone action and that lowering the temperature reduces the rate of membrane remodeling and thus may provide a means to monitor the processes of endocytosis and the mechanisms responsible for water channel retrieval.

The fate of endosomes or the water channels, containing possible aquaporins, concurrent with endocytosis, was investigated using the techniques of TEM combined with undialyzed and dialyzed HRP in toad urinary bladder under an imposed osmotic gradient. Endosomes induced under experimental conditions expressed a variety of sizes containing HRP reaction products with predominant spherical shape while dialyzed HRP produced relatively smaller endosomes compared to undialyzed HRP. Endosomes once internalized into cytosol may enter into trans-golgi network (TGN) for possible reconstitution or become multivesicular bodies or even degrade into lysosomes. Formation and intracellular translocation of endosomes appeared to be depended in part upon phosphorylation of microfilament-associated proteins as wortmannin, a potential inhibitor of myosin light chain kinase, prevented both endosome formation and their intracellular translocation. Many caveolae that occur at the basal plasma membrane of the granular cells internalized HRP when ADH and HRP were added to the serosal bathing solution under an osmotic gradient from serosal to mucosal side. Under these experimental conditions, some HRP-loaded caveolae were found to be involved in transcytosis from the basal to the apical plasma membrane where they fused. Caveolae in toad urinary bladder granular epithelia appeared to be ADH responsive but their role in ADH-mediated water flow process remains to be determined.

INTRODUCTION

Retrieval of Water Channels by Endocytosis in Renal Epithelia

Eukaryotic cells respond with membrane remodeling as part of a number of cellular processes. Exo- and endocytosis are two important cellular mechanisms that are involved in the regulation of enhanced transmembrane osmotic water flow and cycling of water channels in renal and toad urinary bladder granular epithelia following stimulation with vasopressin. Vasopressin induces exocytosis with insertion of water channels (Chevalier et al., 1974; Wade et al., 1981; Kachadorian et al., 1985; Mia et al., 1989; Hays et al., 1994) in concert with propagation of numerous microvilli over the apical membranes of the granular cells (Dratwa et al., 1979; LeFurgey and Tisher, 1981; Mia et al., 1983, 1987, 1988; Mills and Malick, 1978; Spinelli et al., 1975). As a result, the apical membrane undergoes enhanced capacitance (Palmer and Lorenzen, 1983) and conformational changes (DiBona, 1983) during enhanced water flow. Following cessation of hormone actions or receptor down regulation, endocytosis restores the apical membrane surface area and water channels are assimilated into the cytosol (Harris et al., 1986; Coleman et al., 1987; Ziedel et al., 1992, 1993; Mia et al., 1994). Little information exists concerning the effect of temperature on exo- and endocytosis at the apical membrane and its corresponding changes in the cytoplasmic ultrastructure during ADH-mediated water flow.

Previously, we reported preliminary findings concerning time-dependent experimental induction of endocytosis and apical membrane remodeling at two temperatures (25°C and 15°C) that corresponded with the rate of water flow in ADH-challenged toad urinary bladders (Mia et al., 1995, 1998a). Since endocytosis is a highly regulated process and is sensitive to temperature changes (Romagnoli and Herzog, 1994), we conducted the current series of experiments at 25° and 15°C to determine the effects of temperature on membrane remodeling accompanying ADH action in toad urinary bladders. Poikilothermic animals, like amphibians, must adapt to changes in temperature rapidly during normal life cycles as well as during periods of hibernation. This adaptation must include the ability of the animals to osmoregulate under varied temperatures. Experiments were therefore conducted to analyze the effect of lowering temperature to 15°C on endocytosis and water flow, as well as the number and size of membrane invaginations seen following stimulation and removal of vasopressin.

The process of endocytosis, following cessation of hormone action, is believed to be involved in recovering portions of the inserted apical membrane aggrephores or the water channels (aquaporins) as endosomes back into the cytoplasm (Muller et al., 1980; Masur et al., 1984; Wade et al., 1981; Coleman et al., 1987; Ding et al., 1985, 1988; Coleman and Wade, 1994). The characteristics of these aggrephores or the water channels and their fate, as they are internalized as endosomes within the cytosol, have not been fully resolved. In several studies using the fluid-phase marker, HRP (Masur et al., 1972; Coleman et al., 1987, 1994), endosomes containing HRP reaction products were characterized to be in the forms of tubules, vesicles and dense bodies while by others, endosomes were reported to be clathrin-coated pits and vesicles (Franki et al., 1986; Ding et al., 1988; Hays et al., 1994). We therefore, investigated the fate of endosomes (or perhaps water channels) using undialyzed as well as dialyzed HRP in combination with ultrastructural techniques to clarify the morphological identities of endosomes and their fate upon entrance into cytosol (Mia et al., 1998b, c). In addition, how endosomes are delivered into cytosol in toad urinary bladder renal tissues

(Masur et al., 1972; Coleman et al., 1987) required further evaluation (Mia et al., 1998b, c). It is of interest that damage to the kidney may result in the kidney's inability to reabsorb fluid or respond to circulating hormone. Such effects may cause urinary obstruction leading to a medical emergency. It is known that during obstruction, the collecting tubule is unresponsive to vasopressin thereby impairing the cellular process of fluid dynamics. The current ultrastructural studies involving endocytosis may provide some understandings on the restoration of apical membrane, mechanisms of fluid reabsorption and the ability of the kidney to maximize urinary concentrating ability.

We also conducted studies on the role of the cytoskeletal system associated with endosome translocation during ADH-mediated water flow. Several studies emphasized the involvement of microfilaments and microtubules in enhancing the ADH-stimulated water flow process in toad urinary bladder sacs (Taylor et al., 1973, Hardy and DiBona, 1982; Pearl and Taylor, 1983; Hays et al., 1994). In our studies, we report the role of proteins associated with microfilaments that may play a key role in the phosphorylation of microfilament perturbation in the ADH-stimulated water flow process and induction of endocytosis following withdrawal of ADH during a retrieval period. We have investigated if tyrosine phosphorylation of microfilament-associated proteins is involved in cytoskeletal reorganization which mediates aquaporin (water channels) translocation as well as enhances water transport and activates endocytosis. We have also tested the potential involvement of phosphotidylinositol-3-kinase (PI_3 kinase), a key enzyme that has been shown in non-kidney systems to be involved in protein sorting and vesicle fusion.

During our studies of endocytosis, we identified a large number of caveolae (Mia et al., 1997, 1996) at the basal plasma membrane in toad urinary bladder granular cells. Their presence in significant numbers in granular cells and their response to ADH stimulation in detachment and transcytosis from basal to apical plasma membranes through the cytosol and their apparent fusion at the apical membrane appears to be unique (Mia et al., 1997). Caveolae are membrane microdomain structures that are known to serve a variety of cellular functions including transcytosis (Lisanti et al., 1994; Schnitzer et al., 1994; Predescu et al., 1994, 1997) and the transport of proteins (Milici et al., 1987; Predescu et al., 1997). In addition, hormone-sensitive adenylylcyclase system and G proteins are localized in the subfractions of caveolae (Huang et al., 1997), and these may have possible implications in ADH V_2 receptors involvement in water transport process in renal tissues including the toad urinary bladder, in which ADH actions are cAMP-dependent. The mounting evidence involving caveolar organization and dynamics in various cell types suggest that they may have possible involvement in endo- and exocytosis (Mukherjee et al., 1997), and from our studies, transmembrane osmotic water flow in ADH-responsive toad urinary bladder granular cells (Mia et al., 1997).

MATERIALS AND METHODS

Experimental Tissues:

Tropical toads, *Bufo marinus*, purchased from Carolina Biological Supply Company, Burlington, NC, and from NASCO, FT. Atkinson, WI, were maintained in an aquatic environment at 23°C with continuous irrigation of running tap water, and were fed live crickets biweekly.

Experimental Protocol

Whole Bladder Sacs:

For studying the effect of temperature on endocytosis, toads were doubly-pithed and the urinary hemibladders were removed surgically to set up as sacs as described (Bentley, 1958; Mia et al., 1983, 1994). The bladder sacs were equilibrated in normal Ringer's solution aerated continuously using room air for 15 min at 25±1° or 15±1°C in a thermostatically controlled water bath prior to experimental procedures. The composition of the Ringer's solution remained the same as described in our previous studies (Mia et al., 1994). Identical hemibladder sacs from individual animals served as control and experimental tissues. ADH stimulation for 10 or 15 min at room temperature induces maximum water flow as well as membrane fusion events with a limited response down regulation in toad urinary bladders, whereas prolonged ADH stimulation causes spontaneous apical membrane remodeling and return to a state similar to reactivation. Therefore, for studying the temperature effect on apical membrane remodeling, we have used 15 min ADH stimulation for most of our experiments including the current studies.

Following stimulation of bladder sacs with ADH, both control and experimental bladder sacs received two quick serosal buffer rinses at the appropriate temperature for withdrawal of hormone action and the sacs were then allowed to recover or retrieve for 15 or 30 or 60 min to allow for endocytosis and apical membrane remodeling to occur. These experiments were performed at 25°C and 15°C prior to tissue fixation. Before tissue fixation, osmotic water flow was measured gravimetrically (Bentley, 1958) at various time intervals under different temperatures. For tissue fixation, the whole hemibladder sacs were removed from the ends of the glass tubes and quickly submerged into 2% glutaraldehyde at the matched temperature and subsequently fixed for 1 hr. Following buffer rinses, postfixation was carried out using 1% osmium tetroxide at room temperature for an additional hr. These tissues were then divided into samples for SEM and TEM preparations as described later.

Determination of Percent of Surface Involvement:

For analysis of the percent of cells showing surface invaginations, tissues were selected randomly and scanning electron micrographs were taken at X1,500 and X3,000 magnifications from areas with clear cellular delineations as described previously (Mia et al., 1994). As before, the total number of normal and the invaginated cells for each treatment was counted separately and averaged to show the results in percentages (Graph I).

Internalization of Fluid-Phase Marker HRP in Endosomes:

Several experiments were performed for studying either ADH effects or incorporation of horseradish peroxidase (HRP) into urinary bladder cells through mucosal or serosal sides of the bladder sacs with an imposed osmotic gradient between mucosal to serosal or between serosal to mucosal using 1/10 Ringer's solution. In one set of experiments, bladder sacs both inside and outside were bathed in full-strength Ringer's solution with no imposed osmotic gradient. The experimental bladder sacs received serosal stimulation with 100 mU/ml ADH for 10 min but the control sacs (no hormone) were retained in normal Ringer's solution. We then emptied the mucosal solution from both control and ADH-stimulated bladder sacs and quickly replaced with 1/10 Ringer's solution containing undialyzed HRP (5mg/ml). Following three quick serosal buffer rinses of both control and ADH-stimulated sacs, the bladder sacs were placed in full-strength Ringer's solution and allowed 20 min to recover following removal of hormone. This is called the retrieval period for endocytosis prior to tissue fixation. In the second set of experiments, both sides of the bladder sacs were bathed in full-strength Ringer's solution with no osmotic gradient. Control bladder sacs received only HRP in the serosal bathing solution and the experimental bladders received HRP and ADH, and allowed 20 min stimulation for incorporation of HRP into granular epithelia through the serosal side of the bladders before tissue fixation was accomplished. In the third set of experiments, an osmotic gradient was established from serosal to mucosal side using 1/10 Ringer's solution, and the bladders were exposed to HRP through the serosal bathing solution while stimulating the bladders with ADH for 20 min to determine the movement of caveolae as they endocytose from the basal plasma membrane. The control bladders (no hormone) received only HRP at the serosal bathing solution.

We repeated similar sets of experiments on endocytosis as described above but using HRP dialyzed overnight and a low concentration of ADH at 10 mU/ml, and ADH plus wortmannin to determine if wortmannin inhibits myosin light chain kinase activity and endosome internalization into cytosol. In this set of experiments, control bladder sacs received serosal stimulation with 10 mU/ml ADH but the experimental bladder sacs received serosal stimulation with 10 mU/ml ADH plus 7.5 M wortmannin for 10 min. We then emptied the mucosal solution from both control and experimental bladder sacs and quickly replaced with 1/10 Ringer's solution containing dialyzed HRP (5mg/ml). Following three quick serosal buffer rinses of both control and experimental sacs, the bladder sacs were placed in full-strength Ringer's solution and followed by retrieval for 10 or 20 min for endocytosis.

Tissue Fixation:

Following the experimental procedures for each set, bladder sacs, still suspended at the ends of glass tubes, were transferred to pre-cooled Ringer's solution on ice and the bladders were rinsed internally with cold deionized water containing 5.7% sucrose solution to complete endocytosis. The bladders were emptied and fixed internally with 2% cold glutaraldehyde in PIPES buffer and then externally using the same fixative. Fixation was carried out for 1 hr. Following buffer rinses at room temperature, the mucosal or the serosal side of the bladder sacs were exposed to diaminobenzidine (DAB), as per experimental needs, using 2mg/ml plus 2 ml of 1% H_2O_2 in PIPES buffer for 30 min for producing HRP reaction products.

Tissue Preparations for Electron Microscopy:

Tissue processing for SEM and TEM was carried out as described previously (Mia et al., 1987, 1994). Briefly, for SEM, tissues were dehydrated through a series of acetone and liquified Peldri II for critical point drying. The dehydrated urinary bladder sacs were then submerged into fresh liquified Peldri II, and retained for 1-2 hrs for replacement of acetone with Peldri II. Peldri II within bladder sacs was allowed to solidify at a temperature below 23° C (75° F). Peldri II was then allowed to sublimate in a fume hood to complete critical point drying. These tissues were then mounted on clean aluminum stubs and gold coated in an argon environment using a sputter coater. For comparative analysis, all SEM pictures were taken at X1,500 and at X3,000 magnifications with appropriate increases in the printing images. For TEM studies, fixed bladder sacs were buffer rinsed, minced into small pieces and then processed for embedding in epon for ultrathin sectioning. Tissue blocks were polymerized overnight in an oven at 60°C. Ultrathin sections made with a diamond knife were collected on bare copper or nickel grids and exposed to uranyl acetate and lead citrate for staining and TEM studies. Most TEM pictures were made at X31,500, and others were taken at a variable magnification as required and for accuracy of results.

Freeze Fracture Preparations:

For freeze fracture preparation, bladder tissues, fixed only in 2% glutaraldehyde in PIPES (0.02M), and then received cryoprotection with 30% glycerol. Small pieces of these tissues taken on copper holders were plunged into liquid freon at -190°C in a liquid nitrogen bath for freezing. Frozen tissues were then fractured in a Balzers 400T apparatus at -100°C using a metal knife cooled with liquid nitrogen. The fractured surfaces were etched for 5 or 10 min and shadowed with evaporated platinum at 35° and then coated with evaporated carbon at 0°C. These replicas, quickly removed and coated with 1% collodion while still frozen, digested with 5% Na hypochlorite solution to remove tissues from the replicas. The replicas, washed with deionized water were taken on bare copper grids for TEM observations.

Experimental Set Up with Wortmannin:

Purified isolated toad urinary bladder cells were treated with various concentrations of wortmannin in medium at room temperature for 30-60 min. Cells were briefly centrifuged and homogenized. The cell homogenate was used for assay of MLCK using K-MLC selective substrate. ^{32}Pi incorporated in the absence of calcium and calmodulin was subtracted from that in their presence to yield the phosphorylation of K-MLC peptide. The results of wortmannin dose-dependent treatment were presented in Histogram I.

Immunoelectron Microscopic Localization of Anti-Caveolin and Anti-PKCγ Isozyme:

For immunogold labeling, tissues received fixation with 2% glutaraldehyde as in other cases but without postfixation with osmium tetroxide. Minced tissues were dehydrated through exchanges of graded ethanol and L. R. White resin and then cast into blocks in pure L. R. White (Mia et al., 1991). Tissue blocks were polymerized at 60°C in closed gelatin capsules overnight in a vacuum oven.

Tissue blocks were trimmed and sliced with a diamond knife and ultrathin sections were taken on bare nickel grids to perform localization of caveolin or PKC using anti-caveolin IgG or anti-PKCγ IgG and protein-A gold probes (10 nm). The antibodies were diluted separately using 0.1% BSA in PBS and then filtered through 0.2 μm Millipore filter. Ultrathin sections were pre-absorbed with 0.1% BSA for 10 min prior to immunoantibody and gold labeling. These sections were then exposed separately to anti-caveolin or anti-PKCγ monoclonal antibodies (dilution 1/25 using 0.1% BSA in PBS) for 2 hrs and buffer rinsed for labeling with protein-A gold particles (dilution 1/25 using 0.1% BSA) for additional 2 hrs. Control tissues were similarly treated but without antibodies. Each grid received extensive rinses 5 min each in 10 drops of filtered 0.1% BSA in PBS between treatments. The grids were exposed to uranyl acetate and lead citrate for increasing contrast to view in the TEM.

Detection of PKCα Using Western Blotting:

$LLC\text{-}PK_1$ cultured cells are regarded to be excellent experimental renal tissue model and we used them (passage 18-35) to demonstrate the translocation of PKCα from cytosol to plasma membrane following stimulation with vasopressin and phorbol myristate acetate (PMA). These cells were subcultured in DMEM medium (Gibco Inc. Gaithersburg, MD) containing 10% fetal bovine serum and antibiotics. These cells were starved overnight in serum-free medium prior to experimental use (Dibas et al., 1996).

Cytosolic and plasma membrane fractions of PKCα were then isolated using the procedures outlined below. Cultured cells were washed twice in modified Krebs Hanks buffer (134 mM NaCl, 2.5 mM $CaCl_2$, 24 mM $NaHCO_3$, 5 mM KCl, 1.2 mM $MgCl_2$ and 25 mM Hepes, pH7.4) to remove medium and incubated in fresh Krebs solution for 15-30 min. PMA (200 nM) or vasopressin were added to cells to initiate stimulation. Cells were then pelleted and sonicated in ice-cold homogenization buffer (20 mM Tris-HCl, pH 7.5, 0.5 mM EGTA, 1 mM EDTA, 2 mM dithiothreitol, 20 μg/ml aprotonin, 17 μg/ml PMSF and 20 μg/ml soybean trypsin inhibitor). The homogenate was centrifuged to remove nuclei and unbroken cells. The supernatant was centrifuged 1 hr at 100,00 x g (4°C). The cytosolic and plasma membrane fractions were removed and mixed with SDS-sample buffer for gel electrophoresis. We then carried out western blotting to detect the presence of PKCα in the cytosolic and plasma membrane fractions. Protein samples were separated on 7.5% acrylamide as described (Laemmli, 1970). Gels were equilibated in transfer buffer (192 mM glycine, 20% methanol and 25 mM Tris-HCL, pH 8.3) for 15-30 min at room temperature and electroblotted on nitrocellulose membranes for 75 min at 100 volts using a Bio-Rad electroblotting unit. The membranes were dried at room temperature. Western blotting was performed using Tropix chemiluminescent Kit. Membranes were incubated with anti-PKCα antibodies for 1.5 hr (1 μg/ml). The membranes were incubated with the secondary antibody, goat anti-mouse, for 30 min (dilution 1:10,000).

Loading of $LLC\text{-}PK_1$ Cultured Cells with Fura-2:

$LLC\text{-}PK_1$ were grown in culture media as above and were loaded with fura-2 (1 μM) for 30-60 min followed by washing to remove excess fura-2. Cytosolic Ca^{+2} was calculated from the ratio of fura-2 fluorescence at excitation wavelengths of 340 nm and 380 nm according to equations described by

Grynkiewicz et al., (1985). Vasopressin induced a transient increase in $[Ca^{+2}]i$ that declined to basal levels. The data are representative of a total 30 cells studied.

Methods of Water Permeability Studies:

For these studies, toad urinary bladders were mounted as sacs for measuring water permeability. An osmotic gradient was established between the mucosal and serosal bathing solutions. Drugs were added to serosal and/or to mucosal solution, whereas vasopressin (10 mU/ml) was added to serosal bathing solution. Water flow was measured gravimetrically according to Bentley (1958) and as mg/30 min/sac. Tyrosine kinase inhibitors, as well as inactive analogs were added at varying concentrations to serosal, mucosal and to both serosal and mucosal solutions 30 min prior to vasopressin addition. Peptides, which are impermeable, were introduced intracellularly using liposomes as described below.

Effect of Tyrosine Kinase Inhibitors on Dibutyryl-c-AMP & Vasopressin-Induced Endocytosis:

A semiquantitative estimation of the extent of endocytosis was determined using fluorescein isothiocyanate FITC-conjugated dextrin under various conditions by assaying fluorescence. Toad urinary bladder tissues were stimulated with vasopressin in the absence of an osmotic gradient for 15 min in the presence of 2% BSA at the mucosal site to block nonspecific binding. The mucosal solution was then replaced with 1/10 Ringer's solution containing FITC-dextran (5 mg/ml, Mr= 9400, Sigma) and 2% BSA. Serosal bladder surfaces were then washed three times to remove vasopressin. After 5 min incubation with FITC-dextran, the mucosal solution was then washed three times in ice-cold Ringer's solution containing 2% BSA. Urinary bladder cells were isolated by incubating both sides of the bladders using ice-cold Ringer-EDTA (2 mM) for 2 min. Bladders were hand massaged to detach cells which were paletted and incubated in H_2O to lyse them. The fluorescence in the cell homogenate was measured at excitation 496 nm and emission at 516 nm using Shimadzu spectrofluorometer model FR5000U. Fluorescence readings were normalized by assaying protein concentration of the whole cell homogenate. In the case of inhibitors, tyrosine kinase inhibitors as well as inactive analogs were added 30 min prior to vasopressin addition.

Lipofactamine Model:

Anti-PI_3 kinase antibodies (against catalytic and regulatory subunit separately, Sigma Chemical Co.)(10-25 µg/100-200µl dialyzed overnight against N-Ringer's solution to remove sodium azide) were mixed with lipofactamine (50 µg/25 µl, Gibco Co.) by vortexing for 20 min at room temperature. Isolated urinary bladder cells, set up as sacs, received either lipofactamine alone (50 µl) or lipofactamine/antibodies mixture for 2 hr at room temperature. The bladders were then removed and 1/10 Ringer's solution was added to the mucosal side while the serosal side received N-Ringer's solution. Vasopressin (10mU/ml) or dibutyryl c-AMP (1 mM) was added to the serosal side and water transport was carried out as described earlier.

Drugs:

8-Arginine vasopressin (ADH) was purchased from Sigma Chemical Co., St. Louis, MO. The concentration of ADH used in the current series of experiments was 100 or 10 mU/ml and was added to the Ringer's solution on the serosal side.

RESULTS

Temperature Effect on Membrane Surface Remodeling:

Recently, we reported a time-dependent experimental induction of endocytosis and changes in the rate of transcellular osmotic water flow in toad urinary bladders at 25°C (Mia et al., 1994). Since endocytosis is a highly regulated cellular process and is reported to be sensitive to temperature fluctuation, a series of experiments was completed to evaluate the sequence of morphological events of endocytosis and apical membrane remodeling that occurs following vasopressin treatment and its removal at 25° versus 15°C for 15 or 30 or 60 min. The microstructure changes at the apical membrane surface and the cytoplasm, associated with the effects of temperature and hormone, were assessed using the techniques of scanning (SEM) and transmission electron microscopy (TEM). An SEM image from a control urinary hemibladder sac, fixed instantly in glutaraldehyde upon its isolation from a doubly-pithed toad is presented in Figure 1. This procedure captures the apical membrane morphology in nearly its normal state, showing a flat membrane surface configuration containing predominant microridges. This prominent microridge structure was also shown *in vitro* in control bladder tissues set up as sacs using Ringer's solution with an imposed osmotic gradient. However, the *in vitro* bladder sacs showed some degree of swelling of granular cells due to the imposed osmotic gradient. SEM observations of these control tissues (no hormone) retained in Ringer's solution with an imposed osmotic gradient for 15 min at 25° and 15°C respectively (Figs. 2, 3), showed surface microstructures as predominantly composed of microridges and with no evidence of membrane surface invagination typically indicative of endocytosis, as reported in our previous studies (Mia et al., 1994). Complementary bladder tissue subjected to transmission electron microscopic (TEM) studies displayed the cytoplasmic profiles as composed of dense secretory granules, mitochondria and microfilaments with basolateral membranes containing slight indentations with intact desmosomes. Little or no apparent difference in cytoplasmic profile was found as was similarly reported in earlier studies (Mia et al., 1983). Repeating this experimental procedure at 15°C with a 15 min recovery period in control tissues (no hormone) produces no marked discernable morphological differences to 25°C. Figure 4 represents a TEM image of a control tissue retained in Ringer's solution at 15°C following the 15 min recovery period showing typical cytoplasmic profile. The electron dense secretory granules (curved arrows) appear scattered within the cytoplasm mingled with mitochondria (arrowheads), rough ER cisternae (short arrows), golgi body (long arrow), a multivesicular body (b), microtubule and evenly distributed microfilaments. The slightly indented basolateral membranes with intact desmosomes (d) and nucleus (n) appear normal for the control toad urinary bladder tissues. In contrast, toad urinary bladder sacs stimulated with 100 mU/ml ADH for 15 min at 25° or 15°C when examined in the SEM showed propagation of numerous microvilli over the apical membranes as presented in Figures 5 and 6 (arrows) respectively. At 25° or at 15°C during 15 min exocytosis, ADH-stimulated tissues may undergo some endocytosis as depicted by shallow depressions over the apical membranes (arrows) and separations of the basolateral membranes of the granular cells (Figure 7). Analysis of the apical membrane surfaces made from SEM micrographs representing both control (n=6) and ADH-stimulated (n=6) tissues at 25° and 15°C indicated no more than 10% of the granular cells showed evidence of surface membrane invaginations in ADH-challenged tissues during 15 min of treatment at 25° or 15°C, whereas control tissues showed none (Graph I). Osmotic water flow was significantly increased in ADH-stimulated tissues as compared to control tissues during this 15 min stimulation period (Table I). These findings appear to correlate with results from previous studies showing no

more than 15% of the granular cells with membrane invaginations at room temperature (25°C). Ultrathin sections of tissues stimulated with ADH for 15 min at 15°C revealed a cytoplasmic composition with a distribution of secretory granules, mitochondria and other subcellular organelles with evidence of separations of basolateral membranes (Fig. 8, arrows).

The above studies of hormone treatment and exocytosis were complemented with studies of endocytosis following washout at the corresponding temperatures and time periods of 25° or 15°C for 15, 30 and 60 min post washout periods. The control and ADH-exposed tissues, following membrane remodeling and endocytosis of water channels during retrieval periods, were subjected to SEM studies. Figure 9 represents an example of SEM images showing invaginations at the apical surface with a loss of membrane microstructures in ADH-exposed tissues during the 15 min recovery period at 25°C. In some cases, the invaginations involved the entire apical membrane surface with a formation of large cavities as shown in Figure 10. Ultrathin sections show considerable cellular reorientation producing large inter- and intracellular cellular vacuoles (Fig. 11, v). The basolateral membranes were not found to be separated at points where desmosomes were present (Fig. 11, arrows). As a result of compression of the basolateral membranes, intracellular organelles including the microfilaments may become highly condensed within the cytoplasm (Fig. 11, arrowheads). However, the apical membrane disposition of the control toad bladder sacs at the corresponding temperature of 25°C during a 15 min recovery period, showed predominant microridge structure very similar to the structure of the control tissues before washout (Fig. 12) and a general lack of invaginations indicative of endocytosis. Control tissues at 15°C at the 15 min washout period showed some degree of apical membrane invagination (Fig. 13, arrow) while maintaining the predominant microridge structure. However, in some instances, control tissues showed some degree of surface invagination during a 15 min recovery period at 15°C (Fig. 14, arrows), indicating that low temperature had some effect on membrane remodeling. In contrast, ADH-exposed urinary bladder sacs at 15°C at the 15 min retrieval period showed a dramatic expression of surface membrane effects with membrane invaginations involving a large number of granular cells (Fig. 15, Graph I). Here the apical membranes of the granular epithelial cells appear to have shallow apical membrane depressions without truly sequestering the apical membranes into large vacuoles or endosomes as appeared in tissues at 25°C (Mia et al., 1994). Water flow in these tissues remained considerably elevated compared to other ADH-challenged tissues at 25°C (Table I), indicating that the water channels may not have all been internalized as endosomes during this washout period at the lower temperature. A closer SEM view further amplifies the shallow apical membrane profiles with associated short microvilli and deep caving of the basolateral membranes (Fig. 16). Studies of the ADH-stimulated tissues at 15°C at 15 min recovery period showed that some granular cells underwent considerable reorientation and displacement of the cellular organelles from their normal cellular distribution. Figure 17 represents a TEM image showing ADH-treated tissues at 15°C during a 15 min recovery period showing a narrowing and elongation of the granular cells. As a result, most cellular organelles, including the rough ER and mitochondria, are distributed longitudinally along the long axis of the cells (Fig. 17). Most secretory granules (arrows), as seen in this figure, appear to have been displaced from the sub-apical region deep into the cytoplasm. In some cases, the lower temperature effect on ADH-stimulated tissues at 15°C during the 15 min recovery period caused considerable alterations particularly involving the basolateral membranes (Fig. 18, b). Additionally, microfilaments are seen to have clustered (arrows) between the compressed basolateral membranes. However, the sheer forces of compressions at the basolateral membranes failed to cause a complete separation of the adjacent cells at points of desmosome attachments (Fig. 18, large arrows). These tissues also had accumulation of a large number of electron dense secretory granules in some

granular cells (arrows) as seen in Figure 19. Whereas, the control bladder tissues at 15°C at 15 min washout period, showed a different cytoplasmic composition pattern with a scattered distribution of the cellular organelles including the secretory granules (s), rough ER cisternae (r) and microfilaments (arrowheads) with slightly indented basolateral membranes and with intact desmosomes (Fig. 20, arrow).

We have also evaluated the apical membrane of the control and ADH-challenged toad urinary bladder tissues at 30 and 60 mins following washout at 25° and 15°C. Figure 21 illustrates a global SEM image of the control tissues at 30 min recovery period at 25°C showing a large number of granular (arrows) as well as elevated goblet cells (small arrows) with little or no apparent sign of apical invaginations. Tissues treated with ADH at 25°C following a 30 min retrieval period showed surface invaginations involving a large number of granular cells (Fig. 22). Longer recovery times of 60 min for control tissues at 25° or 15°C revealed almost the same apical membrane surface image as that of other control tissues (see Figs. 12, 21). ADH-stimulated tissues following a 60 min washout period at 25°C showed almost complete apical membrane remodeling back to prehormone states such that less than 9% of the granular cells showed surface invaginations (Fig. 21, arrows). In contrast, ADH-stimulated tissues at 15°C during a similar 60 min washout period showed larger membrane surface invaginations (Fig. 24, arrows) that involved twice the number of granular cells (19%) as that of the of the ADH-stimulated tissues at 25°C (Graph I).

An analysis of the percentage of granular cells both in the control and ADH-stimulated tissues showing surface invaginations at 25° and 15°C during 15 min stimulation and following 15, 30 and 60 min washout periods has been carried out using SEM images (see Graph I). Control tissues retained at 25° and 15°C for 15 min showed no sign of apical membrane surface depression indicative of endocytosis. Whereas the ADH-exposed tissues at the same temperatures at 15 min exocytosis showed nearly 10% of the granular cells with surface invaginations, indicating that even during ADH stimulation, some degree of membrane remodeling occurs that may reflect cycling of water channels during hydro-osmosis. Control tissues at 25° (n=13) and 15°C (n=15) during a 15 min washout period showed some apical membrane remodeling, although involving fewer than 6% and 11% of the cells (Graph I). In contrast, ADH-challenged urinary bladder tissues at 25° (n=17) and 15°C (n=15) during a 15 min retrieval period showed a dramatic effect on membrane invagination, with 44% and 80% of granular cells showing membrane surface invaginations at 25° and 15°C respectively (Graph I). Statistical analysis using an ANOVA and Fischer's PLSD showed that there was no significant difference between any of the controls at either at 25° or 15°C during 15 min exocytosis or at 15, 30 and 60 min washout periods. In contrast, ADH-stimulated tissues showed significant differences ($p<.05$) in tissues at 25° and at 15°C during 15 min recovery period, indicating that cold temperature resulted in an increase or retention in the number of invaginations at the apical plasma membranes of the granular cells. The membrane surface collapse or invaginations appeared to be very shallow at 15°C showing little or no sign of membrane internalization. Therefore, the water channels in the ADH-challenged tissues at 15°C during the 15 min recovery period may not have been internalized into the cytoplasm as endosomes. This may be a reason why we observed a sustained elevated water flow for tissues at 15°C even at 60 min post washout (Table I). SEM observations of the control tissues at 15°C during 30 or 60 min washout, revealed only 2-5% of the granular cells showing signs of endocytosis at the apical membrane surface. This was comparable to control tissues observed at 25°C during 30 and 60 min similar washout periods (Mia et al., 1994). In contrast, ADH-challenged tissues at 25° or at 15°C at the same time periods demonstrated considerable membrane surface invaginations involving a number of

granular cells. The percent of granular cells showing the presence of invaginations over the apical membranes at 25°C (n=5) was over 28% (30 min) and 9% (60 min) (n=5) and at 15°C was over 33% (30 min) (n=7) and 20% (60 min) (n=7) in ADH-stimulated tissues respectively, versus less than 2% (30 min) (n=5) and 6% (60 min) (n=8) in comparable control bladder cells. The results indicate that ADH-stimulated tissues continue to show faster apical membrane remodeling during the 60 min recovery period at 25°C compared to tissues at 15°C (Graph I). For this reason, the rate of water flow at 25°C and at 60 min recovery period was considerably lower than the tissues at 15°C at a similar recovery time (Table I). ADH-stimulated tissues at 15°C during a 30 min recovery period when examined in the TEM showed vacuolated cytoplasmic features along with expanded rough ER cisternae and ruffled basolateral membranes as generally associated with ADH-exposed urinary bladder tissues (Mia et al., 1995). However, cytoplasm in the ADH-stimulated tissues following 60 min washout, even at cold temperature, was found to return almost to a normal state.

We carried out a series of experiments to demonstrate the experimental induction of exocytosis and endocytosis in toad urinary bladders correlated with the rate of transcellular water flow in these tissues at 25°C (Mia et al., 1994) as well as at 15°C (Mia et al., 1998a). These studies, provided us with clear understanding of the time-dependent remodeling of the apical membranes during exo- and endocytosis following withdrawal of hormone vasopressin at different time intervals and at two different temperature conditions. We discovered that the apical membranes of the toad urinary bladders undergo extensive invaginations following withdrawal of hormone with subsequent restoration of the apical membranes almost to a normal prehormone control state.

Additional experiments were conducted to observe the effect of ADH under an osmotic gradient imposed in the opposite direction (serosal hypotonic) as no such ADH effect was ever been demonstrated to understand the relative water transport process during exo- and endocytosis (Candia et al., 1997). In these experiments, the bladders were set up as sacs as in other experiments but the osmotic gradient was established in opposite direction from serosal to mucosal side using 1/10 Ringer's in serosal bathing solution. Under these experimental conditions, the addition of ADH did not enhance water flow but actually decreased the net osmotic water movement (Candia et al., 1997, Table I). Morphological analysis of these toad urinary bladders using the SEM indicated that when the mucosal surface was made hypotonic, as under normal conditions, the apical surface of the mucosal membrane displayed normal surface features with predominant smooth configurations of the granular cells and apparent cellular demarcation with little or no cellular swelling (Mia et al., 1983). However, under serosal hypotonic conditions with serosal to mucosal osmotic gradient, the mucosal surface area depicted generalized granular cell (g) swelling and strained cellular junctions (Fig. 25). In the presence of ADH, the granular cells swelled slightly and expressed the typical surface morphology changes seen in response to ADH, ie propagation of apical microvilli from control microridge structure (Mia et al., 1983). However, the granular cells (g) were able to sustain the serosal hypotonicity and there were no further changes in cellular morphology other than swelling and membrane invaginations even in the presence of ADH (Fig. 26).

Endosomes Internalization Using Undialyzed HRP:

This series of studies dealing with endocytosis was directed to determine the fate of the apical plasma membranes as they are internalized as endosomes into the cytosol during membrane remodeling (Mia et al., 1994) following cessation of hormone action or down regulation. These

studies were carried out using the fluid-phase marker horseradish peroxidase (HRP) without or with extensive dialysis to remove non-specific protein components that are present in HRP. These studies allowed us to characterize HRP-loaded endosomes and determine their fate at retrieval periods of 10 or 20 min following hormone withdrawal.

Many transmission electron micrographs were taken using ultrathin sections with or without staining with heavy metals. Unstained ultrathin tissue sections allowed easy identification of endosomes containing HRP and diaminobenzidine (DAB) reaction products within the cellular compartment. Figures 27 and 28 represent comparative TEM images of endosomes in stained and unstained tissue sections respectively. We found endocytosed endosomes of various sizes with predominant spherical in shape (Figs. 27, 28, arrows). Some endosomes appear in association with a large proportion of membrane as shown in a TEM image (Fig. 29, arrows). A portion of these membranes associated with HRP-labeled endosomes must come from the apical membrane and additionally perhaps from membranes of the golgi cisternae upon entrance into trans-golgi network (TGN) compartments. Our previous SEM studies of toad urinary bladders in ADH-challenged tissues at 10, 20, 30 or 60 min recovery period following withdrawal of ADH indicated induction of invaginations at the apical membrane involving a large number granular cells due to endocytosis even at low temperature (Mia et al., 1994, 1998a). This process thus contributes a portion of the endosome membranes as removed during the process of endocytosis. Figure 30 illustrates an example of SEM image (Mia et al., 1994, Fig. 12) denoting apical membrane invaginations correlated with endocytosis and internalization of endosomes at 20 min peak retrieval period. Endocytosis may also induce several invaginations at the same apical plasma membrane as seen in the SEM (Fig. 30, arrows) that may correlate the formation of a cluster of small HRP-loaded endosomes within the cytosol as seen in the TEM images (Figs. 27, 28, arrows). Morphologically, some of these endosome may be regarded to be early endosomes. Some endosomes undergo reconstitution and during interaction with golgi membrane cisternae (Fig. 31, arrows) which can easily be identified by their membrane stacks and associated vesicles. HRP-labeled endosome interactions with golgi cisternae may cause transitional membrane alternations and proliferation.

Following endosome internalization, some appear in transition at or near the apical plasma membrane, while others navigate deep into the cytosol during the retrieval process (Fig. 32, arrows) in tissues following withdrawal of ADH. In ultrathin sections, some endosomes, containing dense vesicular bodies with fine spiny structures and still containing HRP reaction products, appear as multivesicular bodies (MVBs), which are unlike the multivesicular bodies containing internal membrane profiles caused by inward invaginations as previously described (Mukherjee et al., 1997). These multivesicular bodies are normally destined to be degraded by lysosomes for eventual intracellular digestion or to be retained as late endosomes within the cytosol. Some endosomes containing HRP reaction products may transform into late endosomes which obtain characteristics of lysosomes containing HRP reaction products (Fig. 33, arrows). The lysosomes, though heterogeneous in their morphological features, can still be recognized under TEM as spherical bodies containing electron-dense deposits delimited by membranes. These lysosomes may continue to degrade and result in the loss of the endosomal contents leaving only the membrane skeletons (Fig. 34, arrow).

Endosomes Internalization Using Dialyzed HRP:

We carried out similar experiments on endocytosis as described above using dialyzed HRP as a fluid-phase marker and placing within the mucosal cavity for endocytosis to evaluate the nature and formation of endosomes during a 10 or 20 min retrieval period following withdrawal of ADH or ADH plus wortmannin. Figures 35 and 36 represent examples of TEM images taken from unstained ultrathin sections of epon blocks from ADH-stimulated bladder sacs at 10 and 20 min retrieval periods respectively showing several endosomes with inclusions of dialyzed HRP and diaminobenzidine (DAB) reaction products (arrows) within the cytoplasm. Many of the endocytosed endosomes appear to be early endosomes with a predominant spherical shape with few exceptions which appear slightly elongated as shown in enhanced TEM views (Figs. 37, 38, arrows). Endosomes produced by dialyzed HRP in tissues stimulated with 10 mU/ml ADH are essentially smaller compared to undialyzed HRP. Small endosomes may likely occur partly because of removal of nonspecific proteins from HRP and partly due to the use of a lower concentration of ADH. At 20 min retrieval period, few endosomes may transformation into multivesicular bodies occasionally with irregular outline (Fig. 39, arrow) still containing several dense circular bodies and yet others may degrade into lysosomes as seen in unstained TEM sections (Fig. 40, arrow), very similar to those we observed with undialyzed HRP (Fig. 33).

We also tested the role of the cytoskeletal system particularly involving myosin light chain kinase in the formation and intracellular transport of endosomes. Toad urinary bladder tissues, when exposed serosally to ADH containing wortmannin for 10 min and retrieved for 10 or 20 min, showed virtually no internalization of HRP into endosomes. Figure 41 represents an example of TEM images taken from such ADH- and wortmannin-treated bladder tissues from a 20 min retrieval period, showing inhibition of endocytosis with no formation of endosomes and with HRP reaction products localized as dense clouds at the apical plasma membrane (arrows). Wortmannin inhibition of myosin light chain kinase enzyme prevented formation and internalization of endosomes in these bladder tissues. The control bladder tissues under identical experiment conditions with no addition of ADH under an imposed osmotic gradient also caused little or no endocytosis or formation of any endosomes as associated with ADH-stimulated bladder tissues. Dialyzed or non-dialyzed HRP when added into mucosal cavity of the control bladder sacs also remains as deposits of dense HRP clouds at the external apical plasma membrane surface (Fig. 42, arrows) with little or no penetration into cytosol.

Clathrin-Coated Pits and Vesicles in Toad Urinary Bladder Granular Cells:

Several studies on toad urinary bladders indicated the role of aggrephores and vesicles, perhaps coated with clathrin, in endosome internalization. In our studies, we made extensive observation to insure whether receptor-mediated endocytosis involving clathrin-coated pits and vesicles play a major role in apical membrane recovery involving ADH-stimulated water flow process. Numerous TEM images as acquired during our extensive studies of toad urinary bladders showed occasional incidents of clathrin-coated pits at the apical membrane. A TEM image is presented here as an example of rare events (Fig. 43, arrow) to show the presence of a clathrin-coated pit at the apical membrane. However, we observed incidents of clathrin-coated pits at the basal and basolateral plasma membranes (Figs. 44, 45, arrows) of the granular cells but they occur more frequently at the basal plasma membrane than at the apical or basolateral membrane. Clathrin-coated pits may also

detach similarly like caveolae from the basal plasma membrane and migrate to various locations of the cytoplasm as well as to the apical membrane (Fig. 46, arrow) for possible fusion. However, the size of the these coated pits and vesicles is significantly smaller than the HRP-loaded endocytosed endosomes as shown in figure 47 (arrows). An analysis of the relative distribution of caveolae and clathrin-coated pits and vesicles in fifteen TEM images, taken at X8,000 magnification, indicated presence of 87% caveolae as compared to 13% clathrin-coated pits and vesicles. However, neither the caveolae nor the clathrin-coated pits and vesicles appear to be the main pathways of endocytosis through the apical plasma membrane of the toad urinary bladder granular cells. In our many experiments with HRP at the mucosal cavity with an imposed osmotic gradient, we found no evidence of inclusion of HRP into either the caveolae or the clathrin-coated pits and vesicles through the mucosal membrane.

Nature of Endo- and Exocytosis Involving Caveolae in Toad Urinary Bladders:

During our investigation on transmembrane aqueous flow in toad urinary bladders, we discovered the presence of a large number caveolae along the basal plasma membranes of the granular cells facing the cytoplasm. To appreciate the presence of caveolae and their concentration at the basal plasma membrane, a TEM image is illustrated to show how numerous caveolae (Fig. 48, arrows) can possibly alter the ultrastructural details of the basal plasma membrane surface and thus ADH-mediated water flow process.

Immunoantibody and Protein-A Gold Labeling Determination of Caveolin:

Experiments were conducted using specific monoclonal anti-caveolin IgG for detection of caveolin and protein-A gold probes to determine if caveolin (22kd) was the major membrane protein of the caveolae of the toad urinary bladder cells as found in several cultured cell types (Rothberg et al., 1990; Lisanti et al., 1994). Many electron micrographs were prepared to demonstrate the presence of caveolin associated with caveolae in toad urinary bladder. Figures 49 and 50 represent electron micrographs showing immunogold localization of caveolin by the presence of gold particles associated with caveolae (arrows), indicating that caveolin was the major protein component of the caveolae in toad urinary bladders. Control bladder tissues blocked by 0.1% BSA in PBS for 10 min and then exposed to protein-A gold probes showed no localization of caveolin (Fig. 51, arrows).

Dynamics of Caveolae in Toad Urinary Bladder Granular Epithelial Cells:

The presence of caveolae at the plasma membrane of these renal cells, suggest that they may effect water flow process under normal physiological conditions or following ADH stimulation. In addition, we often found detached caveolae, single or clustered, at various locations of the cell including the apical membrane, especially in bladder sacs that received ADH stimulation (Fig. 52, arrows). These observations clearly indicate that caveolae are involved in transcytosis from basal to the apical plasma membranes in toad urinary bladder granular cells. We carried out several experiments using HRP as a fluid-phase marker to determine if caveolae can be induced to incorporate HRP into caveolae through the serosal side of the bladder sacs and migrate from serosal to apical region of the granular cells. In our experiments, we found that many caveolae show HRP

uptake (Fig. 53, arrows) but remained largely anchored at the membrane surface, even in tissues stimulated with ADH with imposed osmotic gradient from mucosal to serosal side. However, if the osmotic gradient was reversed from serosal (serosal hypotonicity) to mucosal direction, many caveolae showed not only uptake of HRP but also detachment from the plasma membrane. As a result, we encountered many HRP-incorporated caveolae free within the cytosol (Fig. 54, arrows) and at locations adjacent to the apical membrane (Figs. 55, 56, arrows) for possible fusion with the plasma membrane. In our freeze fracture replica preparations, we often captured the presence of caveolae at the apical membrane surface in position for fusion (Fig. 57, arrows) especially in bladder sacs that received ADH challenge. Control bladder sacs under an imposed osmotic gradient from either direction of the bladder surface showed little or no inclusion of HRP into caveolae or their detachment from the membrane surface. The experimental evidence of caveolae dynamics indicate that they are vasopressin sensitive and their unique behavior patterns in toad urinary bladder granular cells may have possible roles in ADH-mediated water flow and aquaporin water channel function. Whether caveolae in toad urinary bladder granular cells contribute to water flow regulation mediated by ADH remains to be determined.

Role of Protein Kinase Cγ in Caveolar Transport:

Protein kinase C, a calcium and phospholipid-dependent protein kinase, exists in various isoforms in a variety of tissues and is known to play a key role in the regulation of a variety of intracellular processes including internalization of caveolae (Parton et al., 1994). Protein kinase Cα was also found to be an integral plasma membrane component of caveolae responsible for causing invagination (Smart et al., 1995). The toad urinary bladder tissues when challenged with mezerein (MZ, 10^{-6}M), an activator of protein kinase C for 10 min, and later exposed to anti-PKCγ IgG antibody and protein-A gold particles using ultrathin sections, showed localization of gold particles surrounding the caveolae as shown in figure 58 (arrows). This figure demonstrates a cluster of caveolae, laced with gold particles, deep into the cytosol as well as at the apical plasma membrane, indicating the association of PKCγ with caveolae and PKCγ may be involved in activation and translocation of caveolae.

Results of Western Blotting:

As described that we also investigated the involvement of protein kinase Cα in vasopressin-induced effects on renal water reabsorption using culture renal model LLC-PK_1 porcine kidney cells. Activation of PKCα can be detected by its translocation from the cytosol to the plasma membrane. In LLC-PK_1 cells, the redistribution of PKCα, a predominant isoform of PKC detected, was studied utilizing western blotting after stimulation with vasopressin. Here we present these results of western blotting on LLC-PK_1 cultured cells. As shown in figure 59 that vasopressin treatment failed to affect PKCα redistribution from the cytosol to the plasma membrane. The result indicated that vasopressin (100 mU/ml) failed to induce a translocation of PKCα from the cytosol to the plasma membrane. By contrast, phorbol myristate acetate (PMA, 200 nM), a potent activator of PKC like mezerein (MZ), induced a relocalization of PKCα from the cytosol to the plasma membrane (Fig. 60). After 2 hrs of treatment of cells with PMA, PKCα was predominantly detected in the plasma membrane and absent from the cytosol. These results suggested that the signal transduction pathway

of vasopressin in LLC-PK_1 cells did not involve PKCα activation and translocation. However, vasopressin at the same concentration increased $[Ca^{+2}]i$ (as judged using the fluorescent Ca^{+2}-sensitive dye fura-2 as shown in figure 61 (arrows indicate the times of addition of vasopressin. Therefore, the increase in $[Ca^{+2}]i$ appeared to be a separate event that was not associated with PKC activation. This result was also confirmed by the lack of IP_3 production upon stimulation of LLC-PK_1 cultured cells by vasopressin.

Involvement of Myosin Light Chain Kinase in Endocytosis and Vasopressin-Mediated Water Transport:

A number of reports indicated that cytoskeletal systems involving microfilaments and microtubules operate in renal tissues in the enhancement of water flow mediated by vasopressin. We carried out several experiments to see if other cytoskeletal elements specifically myosin light chains, had any effect on water flow process as well as formation of endosomes in toad urinary bladder renal tissues. Therefore, the involvement of myosin light chain kinase (MLCK) in water transport in toad urinary bladder was investigated. Wortmannin, a potent inhibitor of MLCK, dose-dependently inhibited vasopressin-induced water transport by 55 ± 6% (n=5) at 6 μM, and by 89 ± 2% (n=4) at 60 μM as shown in Histogram I. A similar inhibition was also observed with ML9, another MLCK inhibitor by 57 ± 14% (n=4). In addition, both inhibitors significantly reduced MLCK-induced phosphorylation of K-MLC11-13 peptide (a selective substrate of MLCK), wortmannin inhibited phosphorylation by 89 ± 7% and ML9 inhibited phosphorylation by 77 ± 4% (n=4). Wortmannin and ML9-induced inhibition of water transport was also accompanied by inhibition of endocytosis of fluorescein isothiocyanate dextran (FITC), an endocytic marker. Wortmannin inhibited endocytosis by 66% whereas ML9 inhibited endocytosis by 25% as shown in Histogram II. It is suggested that wortmannin and ML9, inhibitors of water transport, mediate their action at least in part, by inhibition of MLCK and endocytic pathway in toad urinary bladder.

Effect of Phospholipase A2 in the Regulation of Apical Water Permeability in Toad Urinary Bladders:

It has been well documented that vasopressin stimulates production of cyclic AMP which activates a protein kinase (protein kinase A) in the process of increasing water permeability. Activation of PKA is thought to result in the insertion of water channels (aggrephores) into the apical plasma membrane. This fusion of intracellular membrane vesicles to the apical membrane requires the turnover of membrane phospholipids. These lipids are regulated, in part, by activation of cellular phospholipases. The major phospholipases include phospholipase C and phospholipase A2, with each enzyme existing in various isoforms. We examined the effect of phospholipase A2 inhibitors on hormone induced increase in water permeability. Using selective inhibitors of the calcium-dependent and calcium-independent enzymes, we demonstrated that inhibition of PLA2 attenuated both vasopressin-mediated water flow as well as that produced by addition of cyclic AMP (see Table 1). This suggests that the activity of PLA2 is important to the action of vasopressin at a site that is subsequent to the formation of cyclic AMP.

Osmotic water flow was measured gravimetrically (Bentley, 1958) in paired hemibladder sacs in which the gradient was mucosal to serosal in control and experimental tissues. In one set of

experiments, the calcium-dependent inhibitor p-bromophenylacylbromide (BPAB) was added to the serosal bathing solution and water loss was measured. To determine if changes in water flow response to BPAB were at the vasopressin receptor or subsequent to cyclic AMP formation, the same experiment was run but with cyclic AMP as the stimulant. BPAB was found to significantly decrease water flow from 1072 μg/30 min to 243 μg/30 min, suggesting that the action of this inhibitor was after the formation of cyclic AMP. Using another inhibitor of PLA2 activity, HELSS, similar decreases in water transport were observed. These results suggest that PLA2 activity is important to the action of vasopressin and cyclic AMP in increasing osmotic water flow across the toad urinary bladders. PLA2 activity may play a role in the insertion process of water channels into apical membrane.

DISCUSSION AND CONCLUSIONS

The kidney plays a critical role in the reabsorption of water from the urinary side into the systemic circulation, and at times of thirst this is enhanced by antidiuretic hormone (ADH). The process of transcellular enhanced water reabsorption by ADH results from the insertion of water channels into the apical membrane. This ADH effect is seen in many ADH responsive renal tissues, including the toad urinary bladder. Upon serosal stimulation of the toad urinary bladder tissues with ADH, the apical membranes of the granular epithelia become highly water permeable following membrane fusion of water channels during a process of exocytosis. Following exocytosis and the removal of the hormone, the apical membrane undergoes spontaneous recovery and water channels are retrieved into the cytoplasm by a process of endocytosis (Hays et al., 1994; Mia et al., 1994). A number of studies have been carried out to probe the process of endocytosis in toad urinary bladders using fluid phase markers such as horseradish peroxidase (HRP), fluorescent dextran, as well as colloidal gold techniques with applications of transmission electron microscopy (Coleman et al., 1987; Ding et al., 1985; Harris et al., 1986; Muller and Kachadorian, 1984; Zeidel et al., 1992, 1993). While these studies have contributed toward our understanding of the process of retrieval of water channels as related to endocytosis, little information was obtained about the time-dependent membrane remodeling that occurs following removal of the hormone. In addition, little is known about the phenomena of apical membrane restoration during endocytosis at lower temperatures (Mia et al., 1995). In our previous studies, we described the behavior of the apical membranes of toad urinary bladder granular epithelia under various time-dependent experimental conditions during exo- and endocytosis (Mia et al., 1983, 1987, 1994, 1995). These studies were carried out at laboratory room temperature conditions of 25°C with or without the stimulation by ADH. We observed that during hormone stimulation and exocytosis, ADH-stimulated tissues showed minimal signs of apical membrane remodeling in the form of surface remodeling (Mia et al., 1994, 1995). However, ADH-stimulated urinary bladder tissues, following washout, had extensive membrane surface invaginations indicative of surface remodeling. Transmission electron microscopic observations also confirmed the occurrence of large vacuolar compartments within the cytosol concurrent with the apical membrane internalization. To determine if cold temperature could enhance our ability to monitor surface membrane remodeling and water channel endocytosis, we conducted a series of time-dependent experiments of ADH-challenged toad urinary bladder tissues under two different temperatures of 25° and 15°C.

Endocytosis is a highly regulated physiological process that plays a key role in the uptake of macromolecules from the external environment or in retrieving membrane components back into the cell (Mia et al., 1994, Zeidel et al., 1992, 1993, Hansen et al., 1991, Rodman et al., 1990, Rothberg et al., 1990). The process of endocytosis is also found to be temperature sensitive in which decreases in temperature result in the increase in the number and size of endocytic vesicles in thyrocytes and in J774 cells *in vitro* (Romagnoli and Herzog, 1994). In our studies of toad urinary bladders, we observed a dramatic increase in the number of apical membrane invaginations involving a large population of granular cells both at 25° and 15°C during a 15 min post hormone washout period in tissues that received ADH. The number of endocytosed invaginations at 25°C was over 44% versus 80% of cells at 15°C, indicating an increase in the number of invaginations by almost two-fold at the lower temperature. The number of invaginations was found to peak at 15 min post washout as 28% and 33% of the granular cells showed surface invaginations during a 30 min washout recovery period at 25° and 15°C, respectively. Control tissues during a similar 15 min recovery period at 25° and

15°C showed no more than 6% and 10% of granular cells with signs of membrane invaginations, respectively. Whereas during 30 and 60 min recovery periods, control tissues showed less than 3% and 6% of granular cells involved at 25° and 15°C, respectively. These results correlate with our previous studies at 25°C indicating that lowering the temperature to 15°C neither arrested the process of apical membrane restoration nor greatly altered the pattern of apical membrane surface remodeling leading to restoration of the apical membrane to nearly prehormone normal state at 60 min into recovery, though the restoration process appeared to be somewhat slower at 15°C than at 25°C as observed at 30 min retrieval periods.

Previous studies on endocytosis involving toad urinary bladders also indicated an increase in the number and dimensions of the endosomes as determined by HRP and FITC dextran at 10 and 30 min recovery periods (Zeidel et al., 1992, 1993). This increase in the number of endosomes was also found to plateau at 30 min into recovery. Zeidel et al. (1992, 1993) also showed that at 30 and 60 min, the endosomes were larger than 10 min endosomes, whereas the control unstimulated tissues contained no endosomes. Furthermore, they found no functional water channels at 60 min, presumably inactivated or degraded after 60 min following ADH withdrawal (Zeidel et al., 1993). Our current and previous SEM studies on endocytosis of the toad urinary bladder apical membranes under various time-dependent experimental conditions (Mia et al., 1994, 1995) also exhibited almost a complete recovery of the apical membranes into normal state following 60 min washout, with no more than 3% cells showing surface changes. This may indicate that at 60 min following withdrawal of ADH, water channels are largely internalized as endosomes leaving the apical membrane surface virtually water impermeable. Eggena (1972) has also studied the temperature effect on vasopressin action on toad urinary bladder. He also found that although water flow decreased at the lower temperatures the flow was sustained. He also found that the changes in temperature influenced the conformational state of the water channel.

SEM observations demonstrated an increase in the size of the apical membrane invaginations at different temperatures and recovery periods. It was found that there was little difference in the size of invaginations between the control and ADH-stimulated tissues at 25°C during the 15 min post washout recovery periods but at 30 min at the same temperature, we discovered over 34% increase in the size of invaginations in ADH-stimulated tissues compared to control tissues. We also found increases of over 40% and 146% in the size of invaginations in the ADH-stimulated tissues over control tissues at 25° and 15°C at 15 and 30 min of the recovery period. Such a dramatic increase in the size of invaginations at the cold temperature was also reported in cultures of thyrocytes and J774 cells (Romagnoli and Herzog, 1994). However, in the present study, the size of the invaginations was seen to considerably reduce following 60 min washout of ADH both at 25° and 15°C, showing the recovery of the granular cells almost to a normal state.

Our observations using SEM and TEM also revealed the collapse of the basolateral membranes due to extreme compression involving many granular cells during recovery periods at 15°C in ADH-stimulated tissues. In addition, we also observed the assembly of a large number of microfilaments associated with basolateral membrane compression at 15°C. At this stage, we have not been able to determine the role of microfilaments and microtubules in apical membrane remodeling. Displacement and compression of the microfilaments, and likely microtubules, along with compressed basolateral membranes may have contributed to the inhibition of water channel endocytosis that was observed at the lower temperature. Several workers (Taylor et al., 1975; 1978; Pearl and Taylor, 1983) reported an involvement of microtubules in the temperature-dependent

inhibition of water flow in colchicine-treated and ADH-stimulated toad urinary bladder tissues. They reported that inhibition of water flow by colchicine was increased by 50% with lowering of the temperature at each 10 degree interval. Pearl and Taylor (1983) also demonstrated an inhibition of water flow in ADH-stimulated toad urinary bladder tissues by cytochalasin B, and this inhibition was attributed to loss of microfilament function caused by cytochalasin B. From these observations, one may infer that microtubules and microfilaments may have a functional role in the induction of apical membrane internalization associated with endocytosis; however, additional studies are needed.

Cellular membranes are powerful biological structures endowed with a remarkable ability to regulate cellular homeostasis balancing interactions between internal and external cellular environments. In the case of the distal kidney cortical cells and the renal membrane model, toad urinary bladder, plasma membranes play critical roles in shuttling membranes and associated proteins in the regulation of water flow process mediated by vasopressin. This water flow process includes two important biological events of exo- and endocytosis as they relate to the cycling of water channels or aggrephores in vasopressin-sensitive tissues. The exocytic process occurs following hormone stimulation and involves selective packaging of water channels (aquaporins) containing vesicles (aggrephores) for export toward the apical membrane where they fuse (Kachadorian et al., 1977; Wade et al., 1981; Hays, et al. 1994; Mia et al., 1989). The process of endocytosis occurs following hormone inactivation or membrane down regulation and when urinary concentration ability is maximized. During this period, endocytosis allows recovery of the apical membrane perhaps containing water channels back into the cytosol as intact water channels or endosomes. The fate and characteristics of the putative water channels or endosomes in toad urinary bladders, once internalized into cytosol, are not clearly understood (Masur et al., 1984; Franki et al., 1986; Coleman et al., 1987, 1994; Hays et al., 1994). The current investigation was undertaken to answer some of the key concerns pertaining to cycling of water channels, aggrephores or endosomes involving the process of endocytosis (Mia et al., 1998b. c).

Endocytosis is a complex biochemical process (Mukherjee et al., 1997; Dibas et al., 1998) with four distinct pathways known to contribute to this process: receptor-mediated involving clathrin-coated pits and vesicles, bulk-phase involving endosome internalization, phagocytosis and potocytosis utilizing caveolae as vehicles for internalization of small molecules through apical membranes. It has been reported that caveolae are also engaged in transcytosis (Lisanti et al., 1994; Schnitzer et al., 1994; Predescu et al., 1997) in which plasma membrane microdomain structures transport cargoes of macromolecules and proteins from one membrane domain to another. We reported that caveolae in toad urinary bladder granular cells, were involved in unidirectional flow of membrane perhaps containing water channel proteins from basal to the apical plasma membranes (Mia et al., 1997). It has been well understood that bulk-phase endocytosis, involving cycling of water channels or endosomes at the mucosal membrane in vasopressin-responsive tissue of toad urinary bladder, is the main pathway in the recovery process (Coleman et al., 1987; Coleman and Wade, 1994; Mia et al., 1998b,c). During our studies of membrane surface substructures using the techniques of SEM, we found that the apical membrane of the toad urinary bladder underwent stages of profound membrane configuration changes associated with the retrieval process of endocytosis, prior to restoration of the membrane to its normal microridge phase (Mia et al, 1994, 1998a). We also found that retrieval process induced many membrane depressions consistently leading to formation of endocytic vacuoles of various sizes that correlate with the recruitment of endosomes during the retrieval period. The current studies on endocytosis using the fluid-phase marker HRP in the TEM, combined with high or low dose of ADH, confirmed these vacuoles as seen in our previous studies,

to be endosomes of various sizes. Our many TEM images, acquired during these experimental studies on endocytosis, indicate that these HRP-loaded endosomes show predominant spherical configuration (Mia et al., 1998b,c) while some having elongated substructures. It has not been determined whether these endosomes truly represent the water channels containing channel proteins or aggrephores that are presumably cycled into the apical membrane and recycled back into cytosol as reported (Ding et al., 1985; Coleman et al., 1987; Hays et al., 1994; Coleman and Wade, 1994). Our correlative SEM and TEM studies using fluid-phase marker HRP in ultrathin sections indicate that many of the cytosolic internalized endosomes are large and involve internalization of large portion of the apical plasma membrane (Mia et al., 1994, 1998a, b, c) and therefore, many of these endosomes may not truly represent aggrephores which are relatively small in size compared to the size of endosomes we report in these studies. Some endosomes, small or large, as they are recruited from the apical membrane during endocytosis, are expected to contain some previously inserted water channels during the process of exocytosis.

There has been a considerable speculation regarding the shape, size and the life span of the endocytosed endosomes containing HRP reaction products, once they are internalized into cytosol. Ultrastructurally, some investigators found them to be essentially tubular while others found them to be tubulovesicular conferring their disposition to be essentially aggrephore or aggrephore-like structures (Masur et al., 19 84; Coleman et al., 1987; Hays et al., 1994). While we found the presence of few endosomes having slightly elongated microstructures, they are essentially spherical in shape as we presented the evidence with support of a large number of TEM images (Mia et al., 1998b, c). The basic spherical morphologic configuration was not found be greatly altered even with variable concentration ADH from 100 mU/ml to 10 mU/ml combined with using non-dialyzed or dialyzed HRP and involving shorter or longer endocytic retrieval duration. The spherical microfeature configuration remains basically unmodified even when they form individual single or clustered endocytosed endosomes. However, the size of endosomes could be altered by using undialyzed or dialyzed HRP and by changing the concentrations of ADH. Whatever their morphologic manifestation could well be, some endosomes must contain water channel proteins as they were incorporated into the apical membrane upon fusion during induction of exocytosis by ADH, concurrent with high magnitude of water flow. Some investigators considered endosomes as they form during retrieval process to be clathrin-coated (Hays et al., 1994) and others considered them to be destined to be multivesicular bodies or lysosomes (Masur et al., 1972; Wade et al., 1981; Masur et al., 1984; Coleman et al., 1987). In our studies, we found HRP-loaded endosomes as retrieved underwent sorting and phases of ultrastructural morphology which relate to early or late endosomes, multivesicular bodies (MVBs) containing spherical dense bodies, lysosomes at stages of degradation of endocytosed products with remnants of membrane skeletons while others were found to be involved in the reconstitution process (Griffiths and Simons, 1986) within the trans-golgi network (TGN). We consider these manifestations of endosomes to be normal in toad urinary bladder granular cells and found the morphology of endosomes to be consistent with observations in various cell types as reported in literature (Mukherjee et al., 1997).

We also carried out investigation about the role of cytoskeletal system involving myosin light chain kinase in endocytic process and in the inhibition of recruitment of HRP-loaded endosomes. Wortmannin, a potent inhibitor of myosin light chain kinase and wortmannin-sensitive phophorylation (Baker et al., 1998), was found to be involved in virtually restricting the formation and internalization of bulk-phase endosomes containing HRP reaction products, indicates a role for myosin light chains in the water flow process.

Regarding the participation of receptor-mediated endocytosis by clathrin-coated pits and vesicles in toad urinary bladder, we found no evidence of HRP-loaded clathrin-coated vesicles other than endosomes produced only by mucosal membrane invaginations through bulk-phase recruitment process. We found the clathrin-coated pits and vesicles in toad urinary bladder granular cells playing insignificant role in ADH-mediated water flow in these tissues. Many ultrathin sections we examined in the TEM showed presence of only few clathrin-coated pits at the apical plasma membrane whereas, they are more frequently present at the basal plasma membrane with few incidents at the basolateral membranes.

During our investigation, we identified the presence of a significant number of caveolae in toad urinary bladder granular cells which appeared essentially at the basal plasma membrane (Mia et al., 1996, 1997) and which we found to be involved in cellular transcytosis. Most caveolae in other cell types, particularly in mammalian endothelial cells, indicate that they are involved in a variety of cellular functions including transcytosis and transport of macromolecules and proteins (Lisanti et al., 1994: Schnitzer et al., 1994; Predescu et al., 1997). In our studies, we found that many caveolae detach by fission from the native plasma membrane in a process of endocytosis to become free vesicles, and then defuse away to various locations of the cytoplasm at sites of the apical plasma membranes where they are found to fuse in a process of exocytosis (Mia et al., 1996). We found that caveolae responded to ADH stimulation as many caveolae were found to be involved in the uptake of HRP from the serosal side of the bladder sacs when HRP was added to the serosal bathing solution. However, caveolae would not detach from the plasma membrane surface. When the bladder sacs were stimulated with ADH with imposed osmotic gradient from serosal to mucosal side, some caveolae showed uptake of HRP as well as detachment from the basal plasma membrane to navigate through the cytosol to the sites of the apical membrane where they fuse. In these cells, we never observed formation of caveolae at the apical plasma membrane. The caveolar phenomenon appears to be unique in toad urinary bladder granular cells. It has been held that caveolae can serve as an alternative endocytic pathways in elicited macrophases (Kiss and Gueze, 1997). Our observations strongly suggest that caveolae in toad urinary bladder granular cells traverse uniditectionally from the basal to the apical plasma membrane. It is anticipated that their fusion at the apical plasma membrane will result in the deposition of new membrane components containing proteins perhaps water channel proteins. Therefore, caveolae in toad urinary bladder granular cells are not engaged in cycling of membranes as postulated in membrane shuttling hypothesis to recover portions of the membrane involving aggrephores. The membranes from caveolae as deposited at the apical plasma membrane could play a role in modulating apical membrane permeability in response to ADH stimulation.

REFERENCES

Baker, S.A., Caldwell, K.K., Pfeiffer, J.R. and Wilson, B.S. 1998. Wortmannin-sensitive phophorylation, translocation, and activation of PLCγ1, but not PLCγ2 in antigen-stimulated RBL-2H3 mast cells. Mol. Biol. Cell, 9:483-896.

Bentley, P.J. 1958. The effects of neurohypophyseal extracts on water transfer across the wall of the isolated urinary bladder of the toad, *Bufo marinus*. J. Endocrin. 17:201-209.

Candia, O.A., Mia, A. and Yorio, T. 1997. Evidence of basolateral water permeability regulation in amphibian urinary bladder. Biol. Cell, 89:331-339.

Chevalier, J., Bourguet, J. and Hugon, J.S. 1974. Membrane associated particles: distribution in frog urinary bladder epithelium at rest and after oxytocin treatment. Cell Tissue Res. 152:129-140.

Coleman, R.A., Harris, H.W. Jr. and Wade, J.B. 1987. Visualization of endocytosed markers in freeze-fracture studies of toad urinary bladder. J. Histochem. Cytochem. 35:1405-1414.

Coleman, R.A. and Wade, J.B. 1994. ADH-induced cycling of fluid-phase marker from endosomes to the mucosal surface in toad urinary bladder. Am. J. Physiol. 267 (Cell Physiol. 36):C32-C38.

Dibas, A., Mia, A.J. and Yorio, T. 1996. Is protein kinase C alpha (PKCa) involved in vasopressin-induced effects on LLC-PK_1 pig kidney cells? Biochem. Mol. Biol. Intern. 39:581-588.

Dibas, A., Mia, A.J. and Yorio, T. 1998. Aquaporins (water channels): Role in vasopressin-activated transport. Proc. Soc. Exptl. Biol. Med. Invited Review. (Accepted).

DiBona, D.R. 1983. Cytoplasmic involvement in ADH-mediated osmosis across toad urinary bladder. Am. J. Physiol. 245 (Cell Physiol. 14):C297-C307.

Ding, G., Franki, N. and Hays, R.M. 1985. Evidence of cycling aggregate-containing tubules in toad urinary bladder. Biol. Cell, 55:213-218.

Ding, G., Franki, N., Bourguet, J. and Hays, R.M. 1988. Role of vesicular transport in ADH-stimulated aggregate delivery. Am. J. Physiol. 255 (Cell Physiol. 24):C641-C652.

Dratwa, M., LeFurgey, A. and Tisher, C.C. 1979. Effect of vasopressin and serosal hypertonicity on toad urinary bladder. Kidney Int. 16:695-703.

Eggena, P. 1972. Temperature dependence of vasopressin action on the toad bladder. J. Gen. Physiol. 59:519-533.

Franki, N., Ding, G., Quintana, N. and Hays, R.M. 1986. Evidence that the heads of ADH-sensitive aggrephores are clathrin-coated vesicles: implications of aggrephore structures and function. Tissue Cell, 18:803-807.

Griffiths, G. and Simons, K. 1986. The transgolgi network: sorting at the exit site of the golgi complex. Science, 234:438-443.

Grynkiewicz, G., Poenie, M. and Tsien, R.Y. 1985. J. Biol. Chem. 260:3440-3450.

Hardy, M.A. and DiBona, D.R. 1982. Microfilaments and the hydro-osmotic action of vasopressin in toad urinary bladder. Am. J. Physiol. 243:C200-C204.

Harris, H.W., Wade, J.B. and Handler, J.S. 1986. Fluorescent markers to study membrane retrieval in antidiuretic hormone-treated toad urinary bladder. Am. J. Physiol. 251 (Cell Physiol. 20):C274-C284.

Hays, R.M., Franki, N., Simon, H. and Gao, Y. 1994. Antidiuretic hormone and exocytosis: lessons from neurosecretion. Am. J. Physiol. 276 (Cell Physiol. 36):C1507-C1524.

Hansen, S.H., Sandvig, K. and van Deurs, B. 1991. The preendosomal compartment comprises distinct coated and noncoated endocytic vesicle populations. J. Cell Biol. 113:731-741.

Huang, C., Hepler, R.J., Chen, L.T., Gilman, A.G., Anderson, R.G.W. and Mumby, S.M. 1997. Organization of G proteins and adenylyl cyclase at the plasma membrane. Mol. Biol. Cell, 8:2365-2378.

Kachadorian, W.A., Casey, C. and DiScala, V.A. 1977. Time course of ADH-induced intramenbrane particle aggregation in toad urinary bladder. Am. J. Physiol. 234, F461-F465.

Kachadorian, W.A., Sariban-Sohraby, S. and Spring, K.R. 1985. Regulation of water permeability in toad urinary bladder at two barriers. Am. J. Physiol. 248 (Renal Fluid Electrolyte Physiol. 17):F260-F265.

Kiss, A.L. and Gueze, H.J. 1997. Caveolae can be alternative endocytic structures in elicited macrophases. Eur. J. Cell Biol. 73:19-27.

Laemmli, U.K. 1970. Nature 227:680.

LeFurgey, A. and Tisher, C.C. 1981. Time course of vasopressin-induced formation of microvilli in granular cells of toad urinary bladder. J. Membrane Biol. 61:13-19.

Lisanti, M.P., Scherer, P.E., Tang, Z.L. and Sargiacomo, M. 1994. Caveolae, caveolin-rich membrane domains: a signaling hypothesis. Trends Cell Biol. 4:231-235.

Masur, S.K., Holtzman, E. and Walter, R. 1972. Hormone-stimulated exocytosis in the toad urinary bladder. J. Cell Biol. 52:211-219.

Masur, S. K., Cooper, S. and Rubin, M.S. 1984. Effect of an osmotic gradient on antidiuretic hormone-induced endocytosis and hydroosmosis in the toad urinary bladder. Am. J. Physiol. 247 (Renal Fluid Electrolyte Physiol. 16):F370-F379.

Mia, A.J., Tarapoom, N., Carnes, J. and Yorio, T. 1983. Alteration in surface substructure of frog urinary bladder by calcium ionophore, verapamil and antidiuretic hormone. Tissue & Cell, 15:737-748.

Mia, A.J., Oakford, L.X., Torres, L., Herman, C. and Yorio, T. 1987. Morphometric analysis of epithelial cells of frog urinary bladder. I. Effect of antidiuretic hormone, calcium ionophore (A23187) and PGE_2. Tissue & Cell, 19:439-450.

Mia, A.J., Oakford, L.X., Moore, T.M., Chang, P.H. and Yorio, T. 1988. Morphometric analysis of epithelial cells of frog urinary bladder. II. Effect of ADH, calcium ionophore (A23187) and verapamil on isolated dissociated cells. Tissue & Cell, 20:19-33.

Mia, A.J., Oakford, L.X. and Yorio, T. 1989. Alterations of surface substructures and degranulation of subapical cytoplasmic granules by mezerein (MZ) in toad urinary bladder epithelia. Proc. Elect. Micros. Soc. Am. 47:916-917.

Mia, A.J., Oakford, L.X., Cammarata, P. and Yorio, T. 1991. Modulation of cytoskeletal organization and cytosolic granule distribution by verapamil in amphibian urinary bladder epithelia. Tissue & Cell, 23:161-171.

Mia, A.J., Oakford, L.X. and Yorio, T. 1994. Surface membrane remodeling following removal of vasopressin in amphibian urinary bladder. Tissue and Cell, 26:189-201.

Mia, A.J., Oakford, L.X. and Yorio, T. 1995. Temperature effects on surface membrane remodeling in toad urinary bladders during endocytosis. Mol.Biol. Cell, 6:96a.

Mia, A.J., Oakford, L.X. and Yorio, T. 1996. Possible transcytosis by three distinct coated pits and vesicles in granular cells in toad urinary bladder. Mol. Biol. Cell, 7:226A.

Mia, A.J., Oakford, L.X. and Yorio, T. 1997. Evidence indicates possible unidirectional flow of caveolae from basal to apical plasma membranes in toad urinary bladder granular cells. J. Mol. Biol. 8:207a.

Mia, A.J., Oakford, L.X., Wood, J., Dibas, A. and Yorio, T. 1998a. Effect of temperature on apical membrane remodeling in ADH-stimulated toad urinary bladder. Proc. Soc. Exptl. Biol. Med. 218:307-315.

Mia, A.J., Oakford, L.X., Dibas, A. and Yorio, T. 1998b. Nature of ADH-induced endosomes in toad urinary bladder granular epithelial cells. Proc. MSA. In press.

Mia, A.J., Oakford, L.X., Dibas, A. and Yorio, T. 1998c. ADH-induced exo- and endocytosis in toad urinary bladder granular cells. Intern. Congr. Elect. Micros. In press.

Milici, A.J., Watrous, N.E., Stukenbrock, H. and Palade, G.E. 1987. Transcytosis of albumin in capillary endothelium. J. Cell Biol. 105:2603-2612.

Mills, J.W. and Malick, L.E. 1978. Mucosal surface morphology of the toad urinary bladder: scanning electron microscope study of the natriferic and hydro-osmotic response to vasopressin. J. Cell Biol. 77:598-610.

Mukherjee, S., Ghosh, R.N. and Maxfield, F.R. 1997. Endocytosis. Physiol. Rev. 3:759-803.

Muller, J., Kachadorian, W.A. and DiScala, V.A. 1980. Evidence that ADH-stimulated intramembranous aggregates are transferred from the cytoplasmic to luminal membranes in toad urinary bladder epithelial cells. J. Cell Biol. 85:83-95.

Muller, J. and Kachadorian, W.A. 1984. Aggregate-carrying membranes during ADH stimulation and washout in toad bladder. Am. J. Physiol. 247 (Cell Physiol. 16):C90-C98.

Palmer, L.G. and Lorenzen, M. 1983. Antidiuretic hormone-dependent membrane capacitance and water permeability in the toad urinary bladder. Am. J. Physiol. 244 (Renal Fluid Electrolyte Physiol. 13):F195-F204).

Parton, R.G., Joggerst, B. and Simons, K. 1994. Regulated internalization of caveolae. J. Cell Biol. 127:1199-1215.

Pearl, M. and Taylor, A. 1983. Actin filaments and vasopressin-stimulated water flow in toad urinary bladder. Am. J. Physiol. 245:C28-C39.

Predescu, D., Horvat, R., Predescu, S. and Palade, G.E. 1994. Transcytosis in the continuous endothelium of the myocardial microvasculature is inhibited by N-ethylamalemide. Proc. Natl. Acad. Sci. U.S.A, 91:3014-3018.

Predescu, S.A., Predescu, D.N. and Palade, G.E. 1997. Plasmalemmal vesicles function as transcytotic carriers for small proteins in the continuous endothelium. Am. J. Physiol. 272 (Heart Circ. Physiol. 41):H937-H949.

Rodman, J.S., Mercer, R.W. and Stahl, P.D. 1990. Endocytosis and transcytosis. Curr. Opin. Cell Biol. 2:664-672.

Rothberg, K.G., Ying, Y., Kolhouse, J.F., Kamen, B.A. and Anderson, R.G.W. 1990. The glycophospholipid-linked folate receptor internalizes folate without entering the clathrin-coated pits endocytic pathway. J. Cell Biol. 110:637-649.

Romagnoli, P. and Herzog, V. 1994. Temperature-dependent size changes of endocytic vesicles. Mol. Biol. Cell, 5:192a.

Schnitzer, J.E., Oh, P., Pinney, E. and Allard, J. 1994. Filipin-sensitive caveolae-mediated transport in endothelium: Reduced transcytosis, scavenger endocytosis, and capillary permeability of select macromolecules. J. Cell Biol. 127:1217-1232.

Smart, E.J., Ying, Y.S. and Anderson, G.R.W. 1995. Hormone regulation of caveolae internalization. J. Cell Biol. 131:929-938.

Spinelli, F., Grosso, A. and de Sousa, R.C. 1975. The hydroosmotic effect of vasopressin: a scanning electron-microscope study. J. Membrane Biol. 23:139-156.

Taylor, A., Mamelak, M., Reaven, E. and Maffly, R. 1973. Vasopressin: possible role of microtubules and microfilaments in its action. Sci. 181:347-350.

Taylor, A., Maffly, R., Wilson, L. and Reaven, E. 1975. Ann. NY Acad. Sci. 253:723-737.

Taylor, A., Mamelak, M., Golbetz, H. and Maffly, R. 1978. Evidence for involvement of microtubules in the action of vasopressin in toad urinary bladder. I. Functional studies on the effects of antimitotic agents on the response to vasopressin. J. Membrane Biol. 40:213-235.

Wade, J.B., Stetson, D.L. and Lewis, J.A. 1981. ADH action: evidence for a membrane shuttle mechanism. Ann. N.Y. Acad. Sci. 322:106-117.

Wade, J.B., McCuster, C. and Coleman, R.A. 1986. Evaluation of granule exocytosis in toad urinary bladder. Am. J. Physiol. 251 (Cell Physiol. 20):C380-C386.

Zeidel, M.L., Hammond, T., Botelho, B. and Harris, H.W. 1992. Functional and structural characterization of endosomes from toad urinary bladder epithelial cells. Am. J. Physiol. 263 (Renal Fluid Electrolyte Physiol. 32):F62-F76.

Ziedel, M.L., Hammond, T.G., Wade, J.B., Tucker, J. and Harris, H.W. 1993. Fate of antidiuretic hormone water channel proteins after retrieval from apical membrane. Am. J. Physiol. 265 (Cell Physiol. 34):C822-C833.

ACKNOWLEDGEMENTS

We sincerely express our thanks to the U. S. Army Medical Research and Materiel Command for supporting this research project #DAMD17-95-C-5086 on "Retrieval of Water Channels by Endocytosis in Renal Epithelia", tenured at Jarvis Christian College (an Historically Black College, HBCU), Hawkins, Texas and at the University of North Texas Health Science Center at Fort Worth (a Majority Research Institution, MRI), Fort Worth, Texas. We sincerely thank Dr. Ralph Francisconi, Director, EP, for helpful evaluation of the project reports and Mrs. Kathy Hackley, Grants Management Specialist, for assistance during the progress of the project. Students and Research Associate deserve special thanks for their excellent technical support involving this research project. The views and opinions and/or findings contained in this report are those of the authors and should not be construed as an official Department of the Army position, policy or decision unless so designated by other documentation.

KEY TO FIGURES

Fig. 1. SEM of control toad urinary bladder fixed immediately upon surgical removal with no experimental manipulation showing the flat surface image of the apical membrane with predominant distribution of microridges. X3,750.

Fig. 2. SEM of control toad urinary bladder retained at 25°C for 15 min in Ringer's solution under an osmotic gradient showing predominant microridges over the apical membrane during exocytosis. X3,750.

Fig. 3. SEM of control toad urinary bladder retained at 25°C for 15 min in Ringer's solution, buffer rinsed and then retrieved for 15 min showing the distribution of microridges over the apical plasma membrane with no apparent sign of endocytosis. X3,750.

Fig. 4. TEM of control toad urinary bladder granular epithelial cells retained at 15°C for 15 min, followed by buffer rinses to allow for a 15 min recovery. TEM shows basolateral membranes with intact desmosomes (d), electron dense secretory granules (curved arrows), mitochondria (arrowheads), rough ER cisternae (short arrows), golgi body (long arrow), nucleus (n) and a multivesicular body (b) within the dense cytoplasmic profile of these cells. X12,500.

Fig. 5. SEM of toad urinary bladder stimulated with 100mU/ml ADH for 15 min at 25°C showing propagation of numerous short microvilli (arrows) over the apical membranes of the granular cells during exocytosis. X3,750.

Fig. 6. SEM of toad urinary bladder stimulated with 100mU/ml ADH for 15 min at 15°C showing the propagation of numerous microvilli (arrows) over the apical membranes of the granular cells during exocytosis. X3,750.

Fig. 7. SEM of toad urinary bladder stimulated with 100mU/ml ADH for 15 min at 15°C showing at times the presence of shallow depressions (arrows) over the apical membranes of the granular cells during exocytosis. X3,750.

Fig. 8. TEM of toad urinary bladder tissue at 15°C showing scattered distribution of cellular organelles along with slight separations of the basolateral membranes (arrows). X6,250.

Fig. 9. SEM of toad urinary bladder stimulated with 100mU/ml ADH for 15 min at 25°C, buffer rinsed and allowed retrieval for 15 min showing invaginations over the apical membranes of the granular cells indicating possible endocytosis. X3,750.

Fig. 10. SEM of toad urinary bladder stimulated with 100mU/ml ADH for 15 min at 25°C, buffer rinsed and then allowed to retrieve for 15 min showing large invaginations over the entire apical membranes of the granular cells during endocytosis. X3,750.

Fig. 11. TEM of toad urinary bladder stimulated with 100mU/ml ADH at 25°C, buffer rinsed and then retrieved for 20 min showing the presence of small and large inter- and intracellular vacuoles (v), condensed microfilaments (arrowheads), reorientation of the cells with a displacement of desmosomes (arrows). X6,250.

Fig. 12. SEM of control toad urinary bladder retained in Ringer's solution at 25°C, buffer rinsed and then retrieved for 15 min showing predominant distribution of microridges over the apical membranes with no sign of membrane invagination and endocytosis. X3,750.

Fig. 13. SEM of control toad urinary bladder retained in Ringer's solution for 15 min at 15°C, buffer rinsed and then retrieved for 15 min showing slight depressions (arrow) over the apical membranes during endocytosis. X3,750.

Fig. 14. SEM of control toad urinary bladder retained in Ringer's solution for 15 min at 15°C, buffer rinsed and then retrieved for 15 min showing the induction of invaginations over the apical membranes due to cold temperature effect during endocytosis. X3,750.

Fig. 15. SEM of toad urinary bladder stimulated with 100mU/ml ADH for 15 min at 15°C, buffer rinsed and then retrieved for 15 min showing invaginations and caving of the basolateral membranes of the granular cells. X1,875.

Fig. 16. An enhanced view of the Fig. 15 showing the detailed microstructure morphology of the apical membranes of the granular cells with invaginations and dwarf microvilli (arrows). X3,750.

Fig. 17. TEM of toad urinary bladder tissue stimulated with 100mU/ml ADH at 15°C for 15 min, buffer rinsed and then allowed to retrieve for 15 min. Micrograph depicts cellular elongation with a caving in the basolateral membranes and a longitudinal distribution of cellular organelles including the rough ER, mitochondria with a displacement of the electron dense secretory granules (arrows) from the sub-apical region to deeper region of the cytoplasm. X6,250.

Fig. 18. TEM of toad urinary bladder stimulated with ADH for 15 min at 15°C, followed by buffer rinses to allow 15 min recovery. Micrograph demonstrates the extensive infoldings of the basolateral membranes (b) with displacements of desmosomes (large arrows) and clustering of microfilaments (arrows) as a result of compression likely caused by ADH treatment at cold temperature at 15°C. X12,500.

Fig. 19. TEM of toad urinary bladder stimulated with ADH at 15°C during 15 min retrieval period following buffer rinses showing an accumulation of a large number of electron dense secretory granules (arrows). X6,250.

Fig. 20. TEM of control toad urinary bladder tissue retained at 15°C for 15 min, followed by buffer rinses to allow for a 15 min recovery. Figure shows the cytoplasmic profile of the cells with a scattered distribution of microfilaments (arrowheads), secretory granules (s), rough ER cisternae (r) and basolateral membranes with slight infoldings and intact desmosomes (arrows). X25,000.

Fig. 21. SEM of control toad urinary bladder retained in Ringer's solution for 15 min at 25°C, buffer rinsed and then retrieved for 30 min showing the global view with tissue swelling under osmotic gradient and no evidence of apical membrane surface invagination indicative of endocytosis. X500.

Fig. 22. SEM of toad urinary bladder stimulated with ADH for 15 min at 25°C, buffer rinsed and then retrieved for 30 min showing the global view of the apical membrane surface invaginations involving a large number of granular cells and making the cells porous. X500.

Fig. 23. SEM of toad urinary bladder stimulated with 100mU/ml ADH for 15 min at 25°C, buffer rinsed and then retrieved for 60 min showing almost complete restoration of the apical membrane with few cells still showing small invaginations (arrows). X3,750.

Fig. 24. SEM of toad urinary bladder stimulated with 100mU/ml ADH for 15 min at 15°C, buffer rinsed and retrieved for 60 min showing retention of shallow invaginations (arrows) likely without retrieving the water channels. X3,750.

Fig. 25. SEM of toad urinary bladder with a serosal to mucosal osmotic gradient for 30 min showing vivid swelling of the granular cells (g) and caving of the basolateral junctions. X750.

Fig. 26. SEM of ADH-stimulated toad urinary bladder with serosal to mucosal osmotic gradient for 30 min showing vivid swelling of the granular cells (g) as compared to that of the control tissues with formation of some apical membrane invaginations. X750.

Fig. 27. TEM of ADH-stimulated toad urinary bladder with retrieval for 20 min showing internalization of endosomes of varying sizes and mainly spherical shape (arrows) loaded with HRP through the mucosal plasma membrane (P) in stained section. X16,000.

Fig. 28. TEM of ADH-stimulated toad urinary bladder and retrieved for 20 min showing internalization of endosomes of varying sizes and mainly spherical shape (arrows) loaded with HRP through the mucosal membrane (P) in unstained section. X16,000.

Fig. 29. TEM of ADH-stimulated toad urinary bladder with 20 min retrieval showing HRP-loaded endosomes (arrows) associated possibly with golgi cisternae (g) in unstained section. X25,000.

Fig. 30. SEM of ADH-stimulated toad urinary bladder with 20 retrieval showing many membrane invaginations (arrows) which may correlate with endosome formation within the cytosol as seen in TEM section. X2,000.

Fig. 31. TEM of ADH-stimulated toad urinary bladder with retrieval for 20 min showing HRP-loaded endosomes (arrows) within trans-golgi network (g) in stained section. X63,000.

Fig. 32. TEM of ADH-stimulated toad urinary bladder with 20 min retrieval showing multivesicular bodies (arrows) near the apical membrane and deep within the cytosol. X63,000.

Fig. 33. TEM ADH-stimulated toad urinary bladder showing HRP-loaded late endosomes (arrows) which may degrade to be lysosomes during retrieval period. X50,000.

Fig. 34. TEM of ADH-stimulated toad urinary bladder showing degradation of a HRP-loaded endosome leaving essentially with membrane skeletons (arrow). X63,000.

Fig. 35. TEM of ADH-stimulated toad urinary bladder with retrieval for 10 min showing endosomes of varying sizes and mainly spherical shape (arrows) loaded with dialyzed HRP through the mucosal plasma membrane (P) in unstained section. X22,500.

Fig. 36. TEM of ADH-stimulated toad urinary bladder at 20 min retrieval period showing endosomes of varying sizes (arrows) loaded with dialyzed HRP through the mucosal membrane (P) in unstained section. X22,500.

Fig. 37 TEM of ADH-stimulated toad urinary bladders with retrieval for 10 and 20 min respectively showing essentially spherical endosomes (arrows) loaded with dialyzed HRP in unstained section.. X71,000.

Fig. 38 TEM of ADH-stimulated toad urinary bladders with retrieval for 10 and 20 min respectively showing essentially spherical endosomes (arrows) loaded with dialyzed HRP in unstained section.. X71,000.

Fig. 39. Enlarged view of the TEM image as in figure 10 showing dialyzed HRP-loaded endosomes (arrow) with irregular shape in unstained section. X71,000.

Fig. 40. TEM of toad urinary bladder stimulated with ADH and retrieved for 20 showing dialyzed HRP-loaded lysosome (arrow) in unstained section. X71,000.

Fig. 41. TEM of ADH plus wortmannin-treated toad urinary bladder with 20 min retrieval period showing inhibition of endocytosis with dialyzed HRP reaction products appearing as dense clouds (arrows) over the apical plasma membrane in unstained section. X75,000.

Fig. 42. TEM of control (no hormone) toad urinary bladder showing HRP reaction products deposited as dense clouds (arrows) over the apical membrane of a stained section. X70,000.

Fig. 43. TEM of toad urinary bladder showing showing a clathrin-coated pit (arrow) which forms rarely at the apical plasma membrane . X56,000.

Fig. 44. TEM of toad urinary bladder showing a clathrin-coated pit (arrow) and caveolae (short arrows) at the basal plasma membrane inner to the basement (b) membrane. X56,000.

Fig. 45. TEM of toad urinary bladder showing the presence of a clathrin-coated pit and caveolae (arrows) at the basolateral membranes. X56,000.

Fig. 46. TEM of toad urinary bladder showing two attached clathrin-coated vesicles (arrows) adjacent to the apical plasma membrane. X100,000.

Fig. 47. TEM ADH-stimulated of toad urinary bladder showing the relative size of a clathrin-coated vesicle adjacent to large HRP-loaded endosome (arrows). X63,000.

Fig. 48. TEM of toad urinary bladder showing the distribution of a large number of caveolae (arrows) at the basal plasma membrane inner to the basement membrane (b). X57,500.

Fig. 49. TEM of toad urinary bladder showing detection of caveolin by anti-caveolin IgG and protein-A gold particles over caveolae (arrows) along the plasma membranes. X63,000.

Fig. 50. TEM of toad urinary bladder showing detection of caveolin by anti-caveolin IgG and protein-A gold particles (arrow) over a caveola. X63,000.

Fig. 51. TEM of toad urinary bladder preabsorbed with 0.1% BSA and then exposed to protein-A gold probes (control tissue) showing no binding of gold particles with caveolae (arrows). X63,000.

Fig. 52. TEM of toad urinary bladder showing caveolae (arrows) at the apical plasma membrane in a granular cell and in positions of fusing with the plasma membrane. X57,500.

Fig. 53. TEM ADH-stimulated toad urinary bladder showing HRP-loaded caveolae (arrows) through the serosal side of the bladder sac under osmotic gradient from mucosal to serosal side. X57,500.

Fig. 54. TEM of ADH-stimulated toad urinary bladder showing HRP-loaded some free caveolae (arrows) through the serosal side of the bladder sac under osmotic gradient from serosal to mucosal side in unstained section. X18,000.

Fig. 55. TEM of ADH-stimulated toad urinary bladder showing caveolae (arrows) near the apical membrane loaded with HRP through the serosal side of the bladder sac under osmotic gradient from serosal to mucosal side in unstained section. X18,000.

Fig. 56. TEM of ADH-stimulated toad urinary bladder sac showing a caveola (arrow) at the apical plasma membrane with loaded with HRP through the serosal side of the bladder sac under osmotic gradient from serosal to mucosal side. X71,000.

Fig. 57. Freeze fracture replica preparation from ADH-stimulated toad urinary bladder sac showing fusion of several caveolae (arrows) at the apical plasma membrane. X45,000.

Fig. 58. TEM of toad urinary bladder showing localization of protein kinase Cγ by anti-PKCγ and protein-A gold probes in association with caveolae (arrows) in the cytoplasm as well as at the apical plasma membrane. X33,500.

Fig. 59. Immunodetection of PKCα redistribution in the cytosolic (c) and plasma membrane (p) fractions of LLC-PK_1 cells after stimulation with vasopressin (100 mU/ml).
Lane 1: control (c), lane 2: control (p), lane 3: vasopressin 3 min (c), lane 4: vasopressin 3 min (p), lane 5: vasopressin 6 min (c), lane 6: vasopressin 6 min (p), lane 7: vasopressin 12 min (c), lane 8: vasopressin 12 min (p). also the effect of vasopressin was followed at shorter times (2 min) and after 15 and 60 min but no relocalization of PKCα was observed. The date are representative of at least 3 different experiments.

Fig. 60. Immunodetection of PKCα redistribution in the cytosolic (c) and plasma membrane (p) fractions of LLC-PK1 cells after stimulation with PMA (200 nM).
Lane 1: control (c), lane 2: control (p), lane 3: PMA 15 min (c), lane 4: PMA 15 min (p), lane 5: PMA 2 hr lane 6: PMA 2 hr (p). There was a clear translocation of the enzyme from the cytosol to the plasma membrane. The data representative of at least 3 different experiments.

Fig. 61. Ratio of fura-2 in vasopressin (100 mU/ml) increased $[Ca^{+2}]i$ in LLC-PK_1 cultured cells.

Table I. Effect of temperature on osmotic water flow recovery following ADH-treatment and washout.

	Period I	Period II		
Temperature	Hormone Treatment	Washout		
	15 min	15 min	30 min	60 min
A. 25°C				
Control	104± 13 (12)	78 ±29 (6)	37± 9 (6)	40± 9 (6)
ADH	851±190 (12)	796±59 (6)	489±92 (6)	172±29 (6)
B. 15°C				
Control	127±15 (12)	79± 28 (6)	71±18 (6)	54±14 (5)
ADH	611±95 (12)	870±176 (6)	*832±56 (6)	*448±66 (5)

The number of experiments are in parenthesis. Water flow as mg/30 min. Represented as means ± S.E.

Period I represents 15 min following treatment with ADH or without ADH.

Period II represents time periods post-washout of hormone.

*$p<.05$ for differences from 25°C treatment using a student's T- Test.

Table II: Water flow across toad urinary bladders under a reversed osmotic gradient

Treatment	Period I Basal Conditions	Period II +ADH (60 min)	Period III + ADH (90 min)
Control -	47 ± 20	969 ± 54	865 ± 57
Experimental - BPAB 25 μM	35 ± 22	511 ± 48*	553 ± 123*

Results as mean +- S.E. of six paired experiments.
*p{0.05 for differences from control.

To determine if changes in water flow response to BPAB were at the vasopressin receptor or subsequent to cyclic AMP formation, the same experiment was run but with cyclic AMP as the stimulant. BPAB significantly decreased water flow from 1072 mg/30 min to 243 mg/30 min, suggesting that the actions of this inhibitor was after the formation of cyclic AMP, perhaps at the PKA water channel site or its fusion. Using another inhibitor of PLA2 activity, HELSS, similar decreases in water transport were observed.

As mg/30 min

Treatment	Period I 45 min	Period II 60 min	Period III 75 min
Control - cyclic AMP	323 ± 12	659 ± 24	485 ± 8
Experimental - HELSS 50 μM	52 ± 2*	67 ± 2*	79 ± 5*

Results as mean +- S.E. of six paired experiments.
*p{0.05 for differences from control.

Conclusions: These results suggest that PLA2 activity is important to the action of vasopressin and cyclic AMP in increasing osmotic water flow across toad urinary bladders. It further suggests that PLA2 activity may be more important to water channel insertion process as inhibitors of its activity have greater effects on cyclic AMP induced water flow.

RESEARCH CONTRIBUTIONS

Received: Diatome Award, Second place at the Microscopy Society of America at Cleveland, Ohio (August 14, 1997) for Best Poster Presentation at the Annual Meeting.

Full-Length Papers Published and Submitted:

i) Is protein kinase C alpha (PKCα) involved in vasopressin-induced effects on LLC-PK_1 pig kidney cells? Biochem. Mol. Biol. Intern. 39:581-588 (1996).

ii) Mechanism of vasopressin-induced increase in intracellular Ca^{2+}($[Ca^{2+}]i$) in LLC-PK_1 porcine kidney cells. Am. J. Physiol. 272 (Cell Physiol. 41):C810-C817 (1997).

iii) The ATP-depleting reagent "iodoacetamide" induces the degradation of protein kinase C alph (PKCα) in LLC-PK_1 pig kidney cells. Life Scis. 61:1697-1704 (1997).

iv) Evidence of basolateral water permeability regulation in amphibian urinary bladder. Biol. Cell, 89:331-339 (1997).

v) Effect of temperature of apical membrane remodeling in ADH-stimulated toad urinary bladder. Proceedings of the Society for Experimental Biology and Medicine. 218:307-315 (1998).

vi) Invited Review: "Aquaporins (water channels): Role in vasopressin-activated transport". Proceedings of the Society for Experimental Biology and Medicine (Accepted, 1998).

vii) Role of caveolae and coated pits and vesicles in endo- and exocytosis in granular cells of toad urinary bladders. In Preparation.

viii) Involvement of Myosin Light Chain Kinase in Vasopressin-Activated Water Transport of Toad Urinary Bladders. (In Preparation).

Abstracts Published and Submitted:

i) Temperature effects on surface membrane remodeling in toad urinary bladders during endocytosis. Mol. Biol. Cell, 6:296a (1995).

ii) Immunofluorecent detection of clathrin in LLC-PK1 porcine kidney cultured cells stimulated with vasopressin and mezerein. NIGMS, 69 (1995).

iii) Presence of caveolae and coated pits in toad urinary bladder granular epithelium. FASEB J. (1996).

iv) Phorbol myristate acetate (PMA) induced protein kinase C translocation in LLC-PK_1 pig kidney cells. FASEB J. (1996).

v) Possible transcytosis by three distinct coated pits and vesicles in granular cells in toad urinary bladder. Mol. Biol. Cell, 7:226a (1996).

vi) Nature of caveolae in the endothelial cells of toad urinary bladders. Proc. Microscopy and Microanalysis, 934-935 (1996).

vii) Evidence indicates possible unidirectional flow of caveolae from basal to apical plasma membranes in toad urinary bladder granular cells. J. Mol. Biol. 8:207a. (1997).

viii) The ATP-depleting reagent "iodacetamide" induces the degradation of protein kinase C alpha (PKCa) in LLC-PK1 pig kidney cells. FASEB J. (1997).

ix) Presence of caveolae in the granular epithelial cells of rabbit urinary bladder. Microscopy and Microbeam Analysis (1997).

x) Nature of ADH-induced endosomes in toad urinary bladder granular epithelial cells. Microscopy Society of America. (1998).

xi) ADH-induced exo- and endocytosis in toad urinary bladder granular cells. International Congress on Electron Microscopy. Cancun, Mexico. (1998).

xii) Effect of vasopressin on endosomes and caveolae in toad urinary bladder granular cells. Research Appreciation Day. University of North Texas Health Science Center at Fort Worth. (1998).

OTHER ACTIVITIES

Training of Students:

Two African-American undergraduate students at Jarvis Christian College received training in biomedical research and career enhancement. These students were involved in culturing LLC-PK_1 cells and maintaining them as well as preparing tissues for fluorescent microscopic studies. They developed excellent skills in using the computers.

Two African-American students, graduates of Jarvis Christian College, continue their graduate studies in biomedical sciences working under Dr. Yorio's mentorship at the UNT Health Science Center at Fort Worth. One of these students will receive their Master's degree in August.

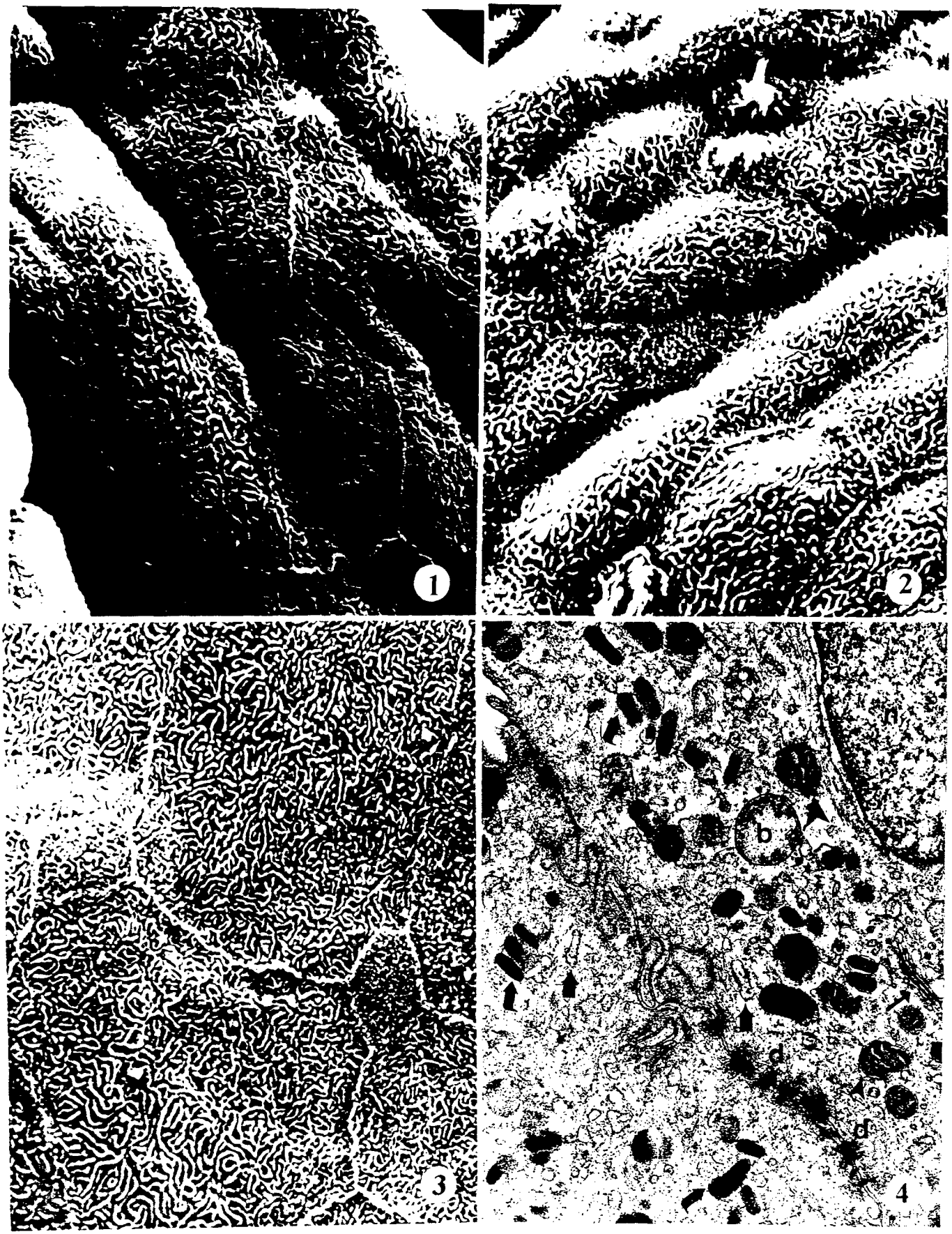
1
2
3
b
d
d
4


5


6


7

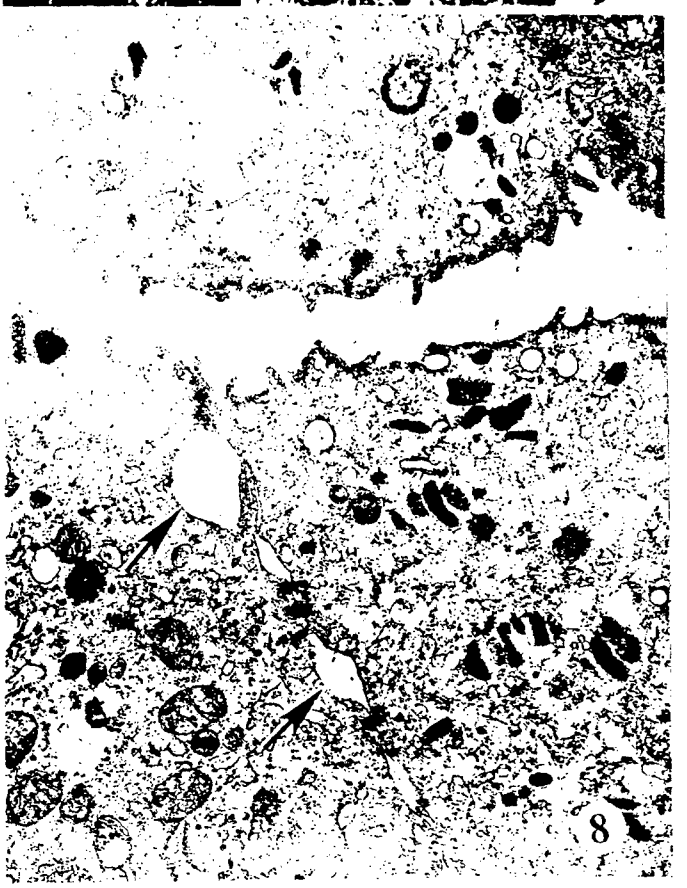
8


9


10


V
V
V
V
11


12

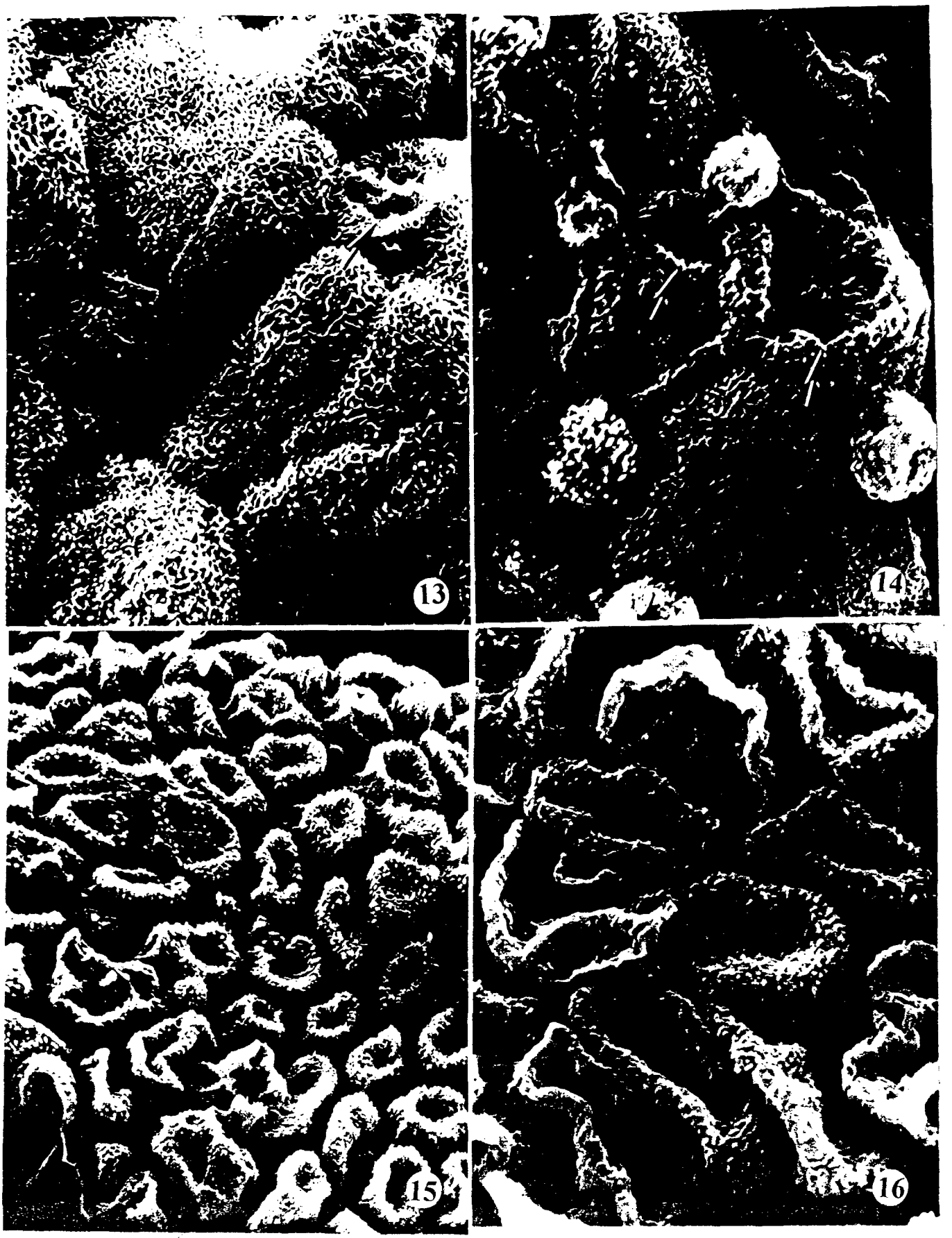
13
14
15
16


17

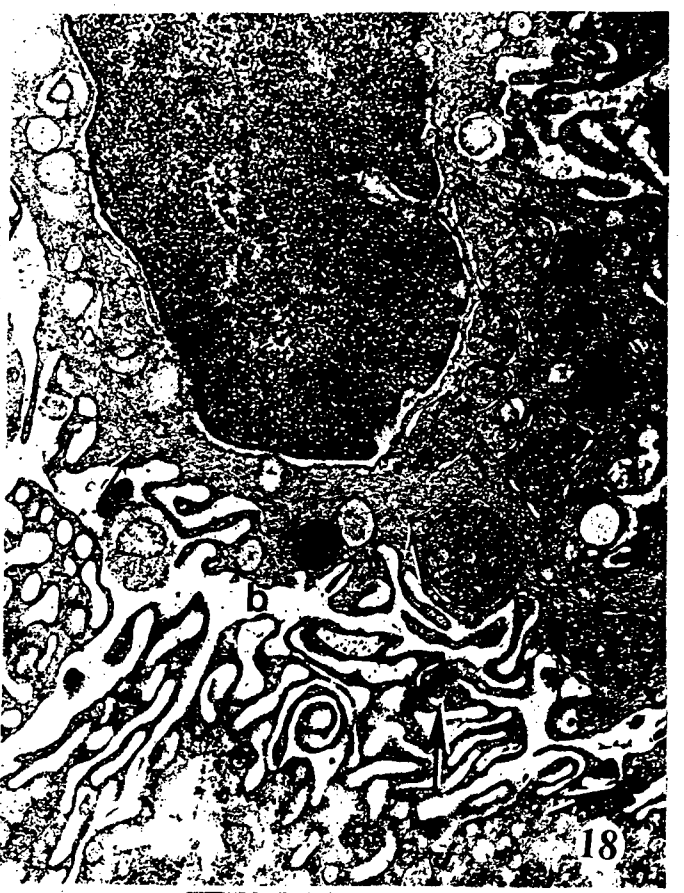
18


19

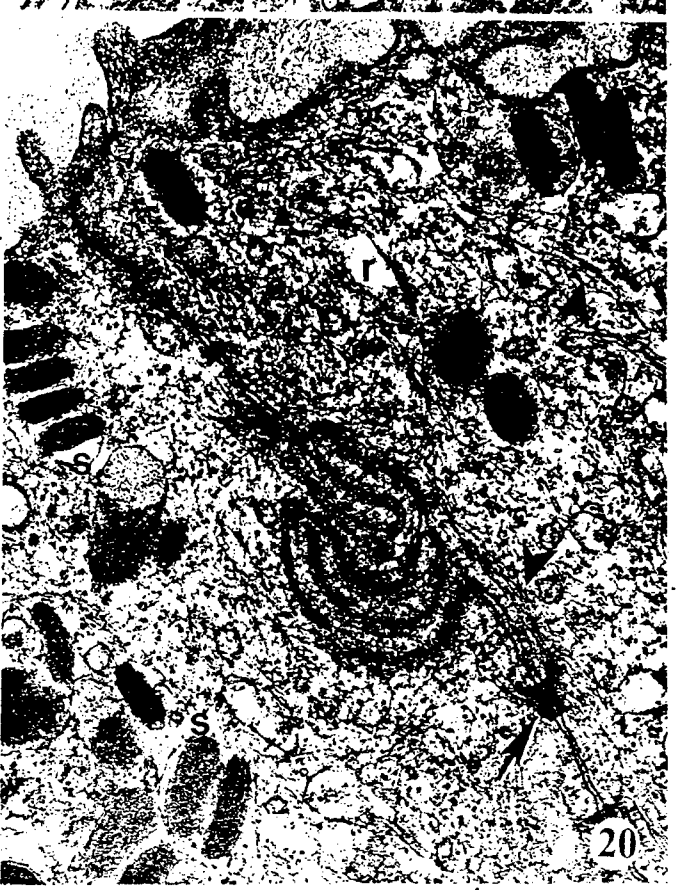

20

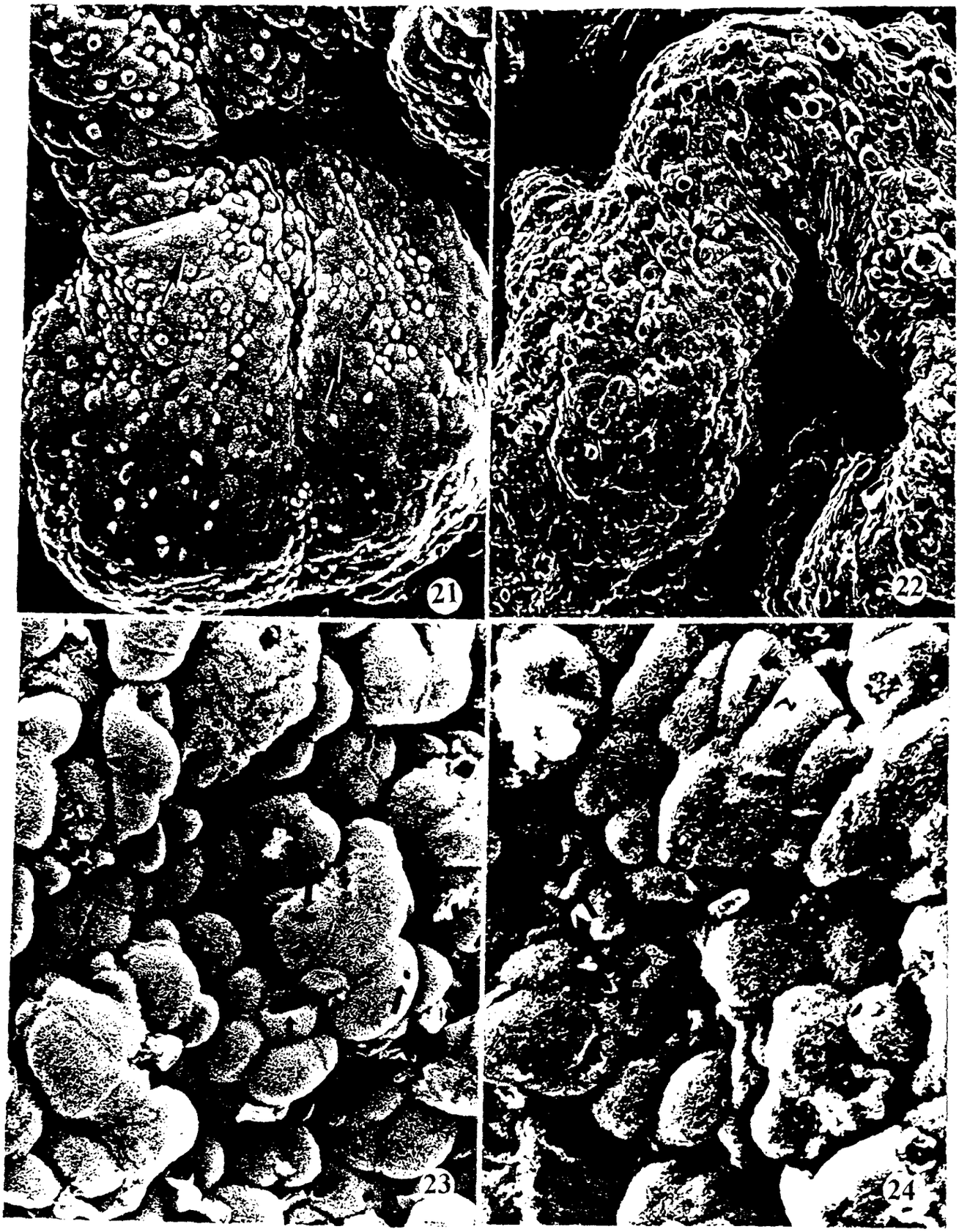
21
22
23
24

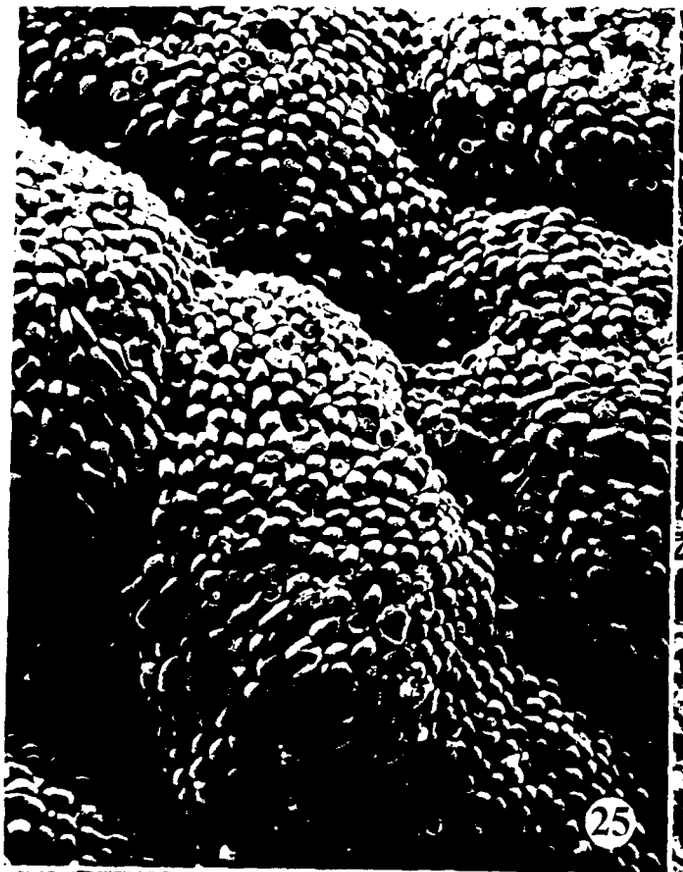

25

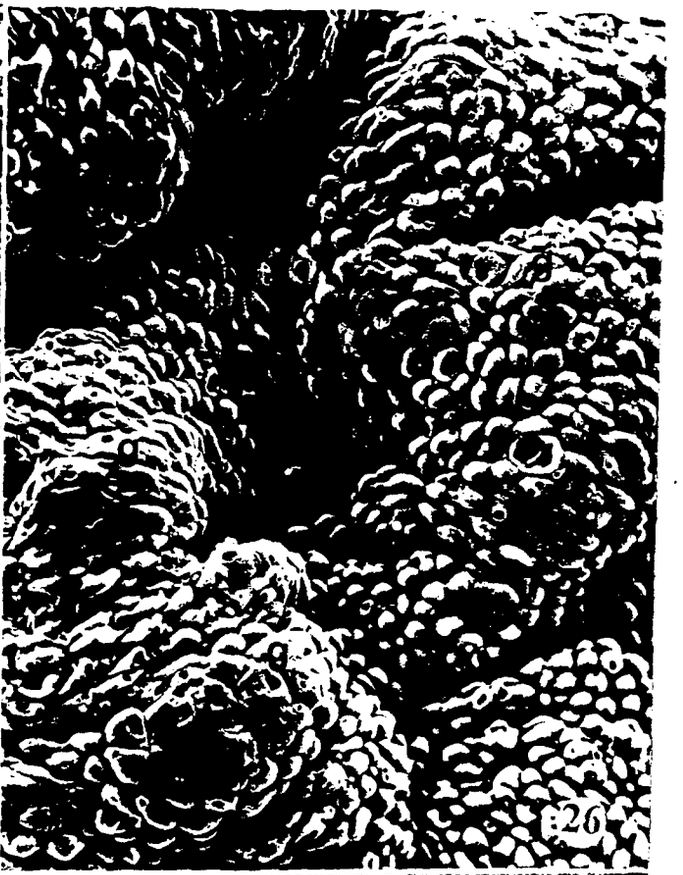

26

27

28

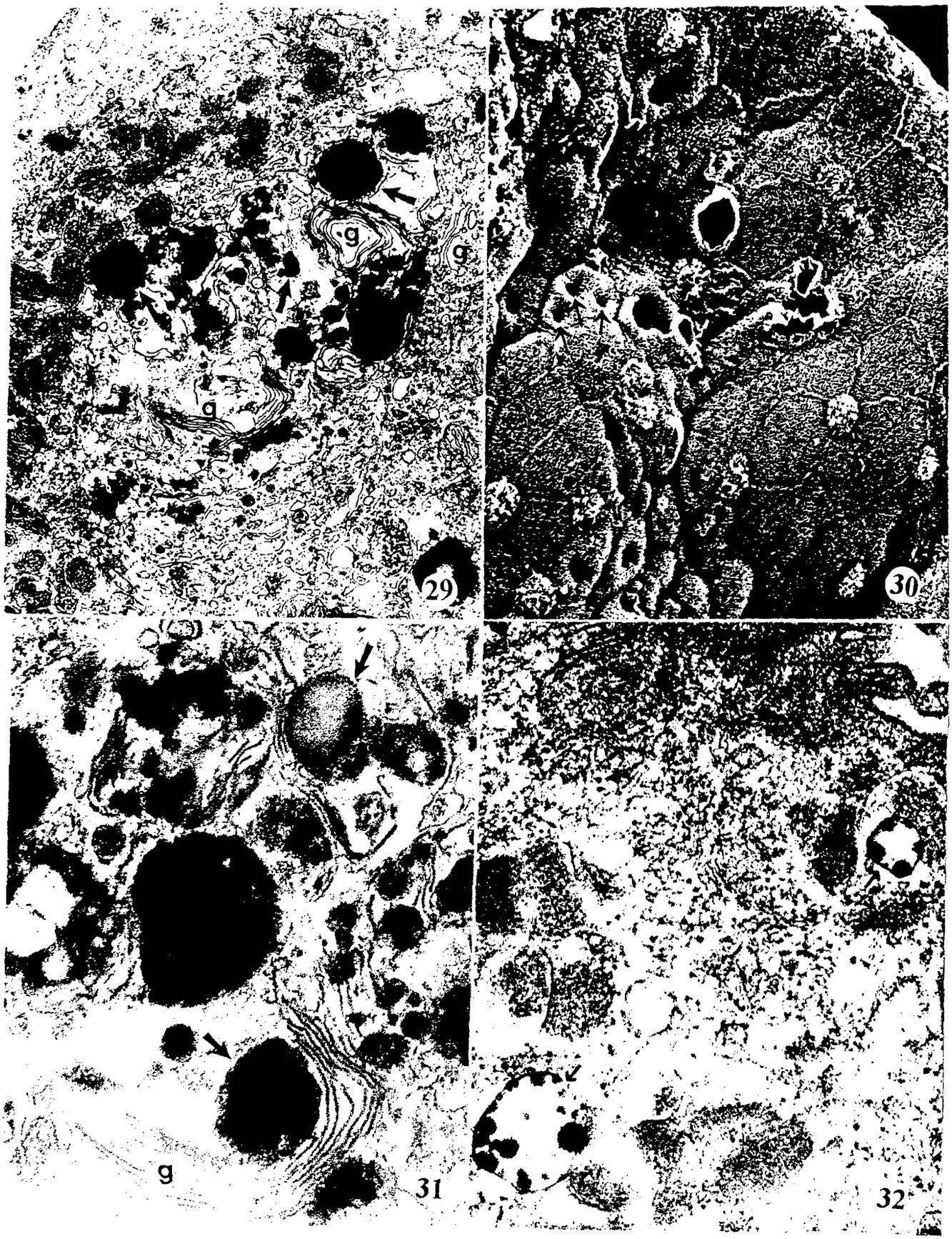
g
g
g
29
30
g
31
32

33

34

35

36

37

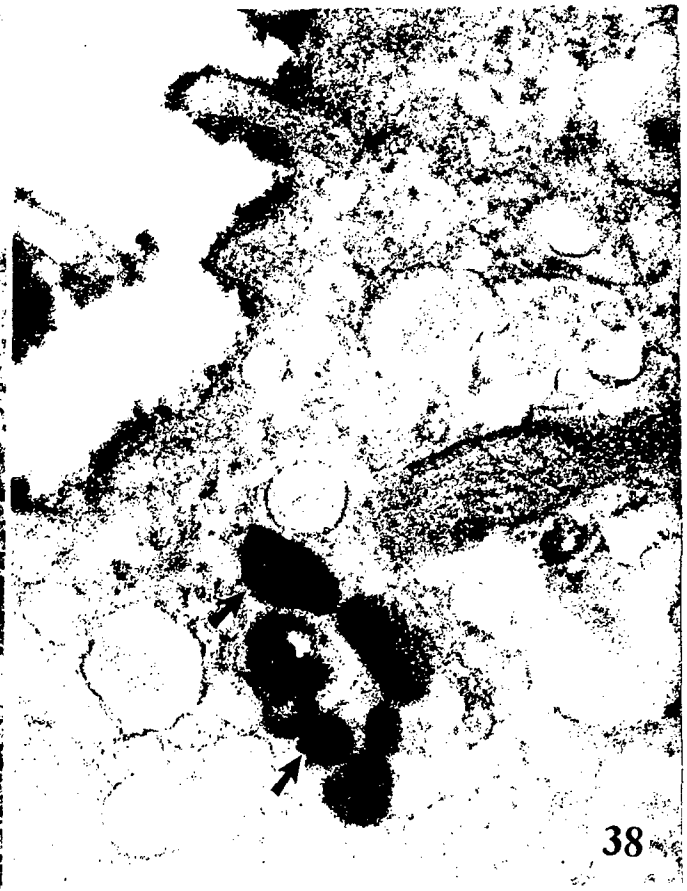

38

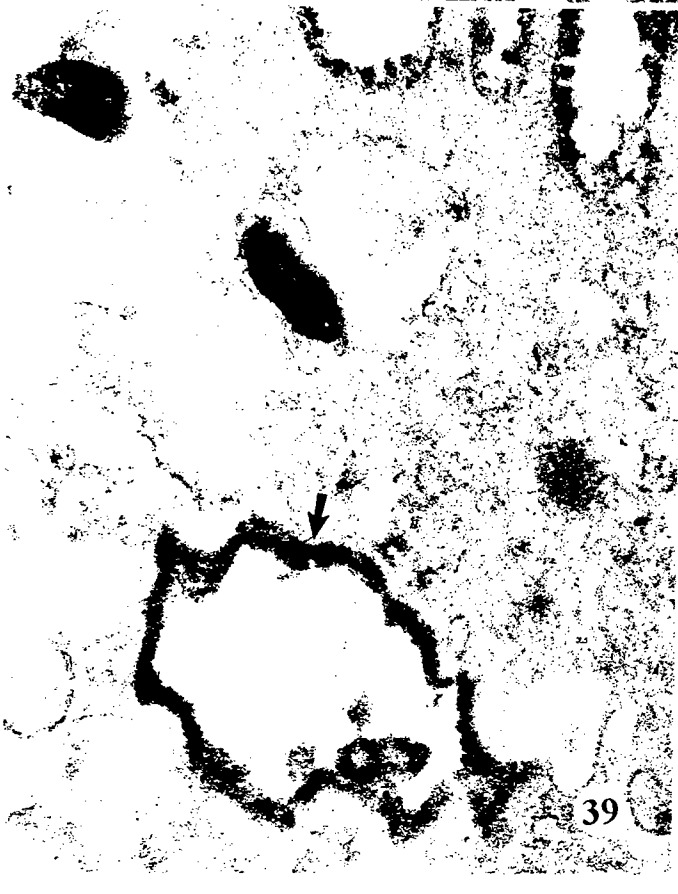

39

40

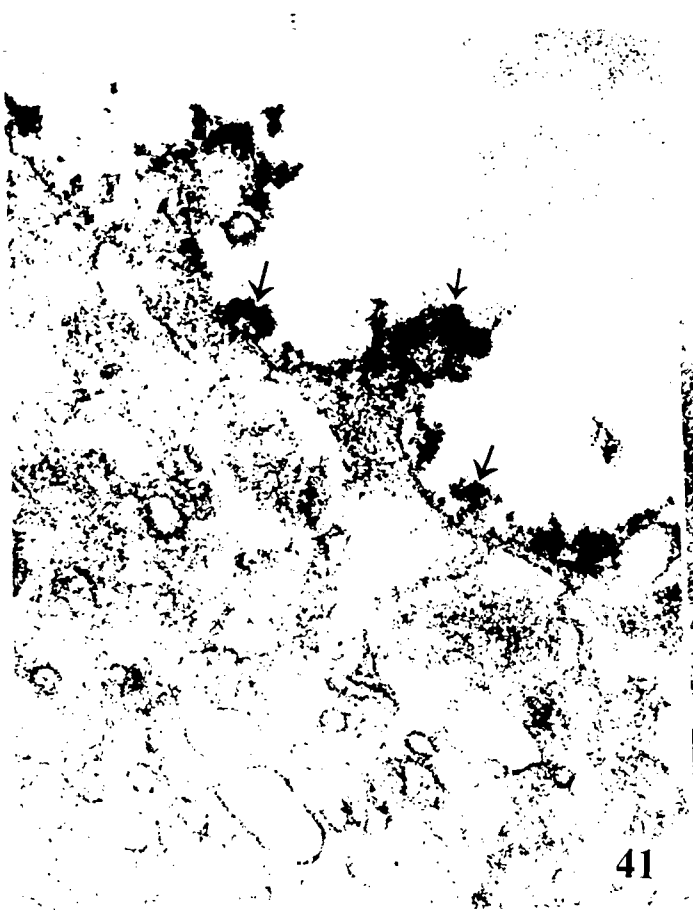

41

42

43

44

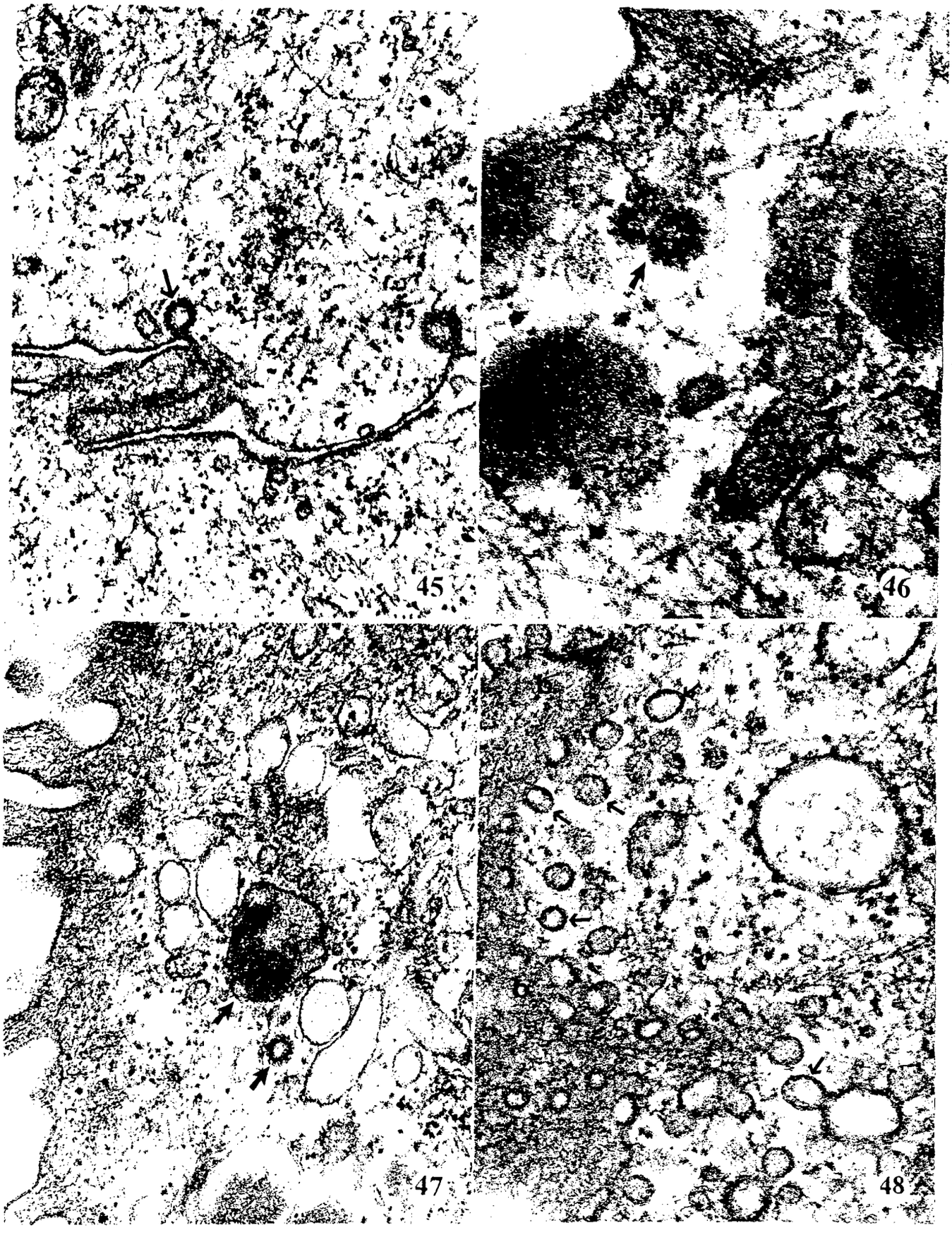
45
46
47
48

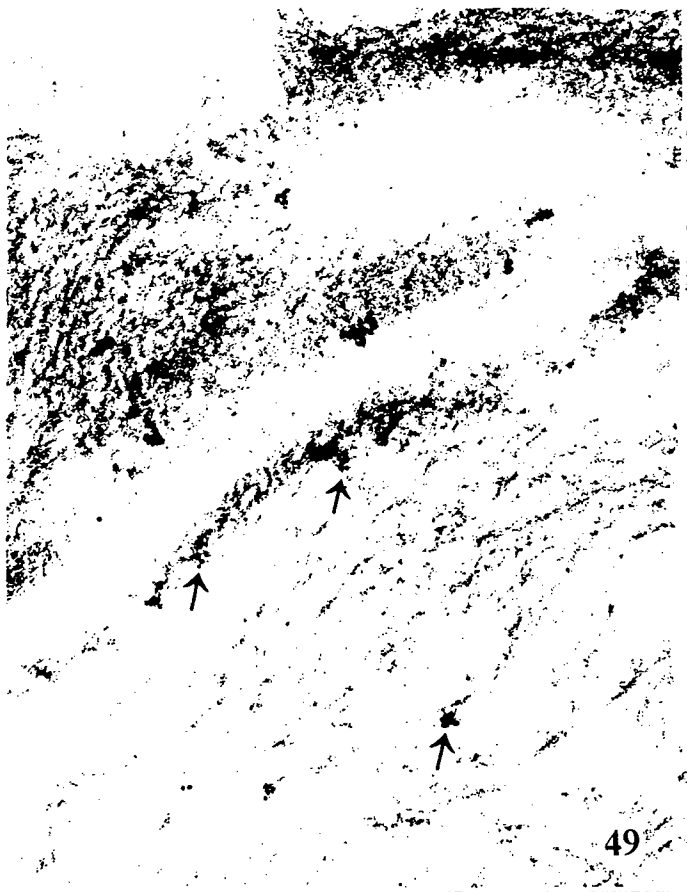

49

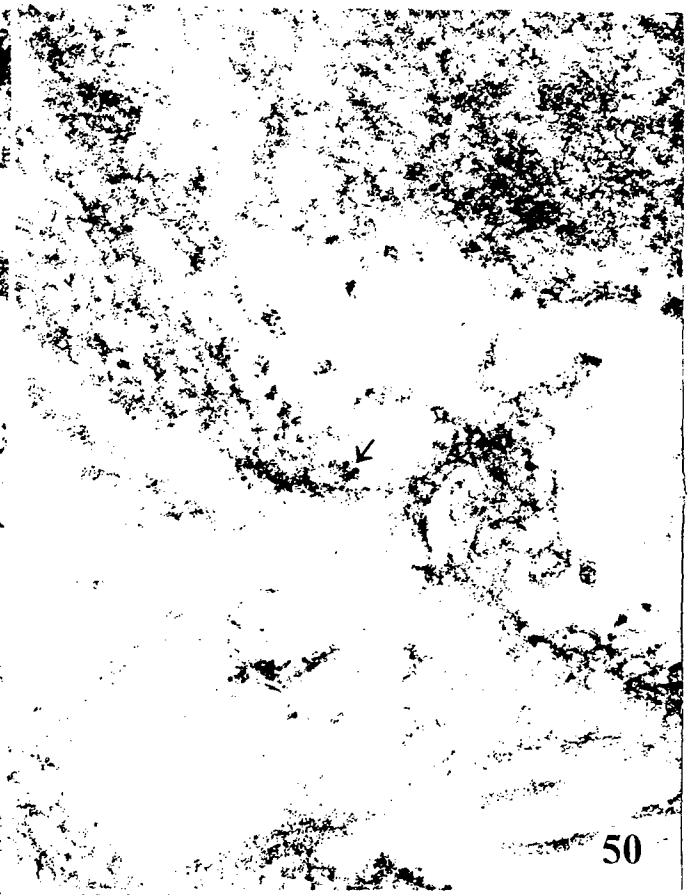

50

51

52

53

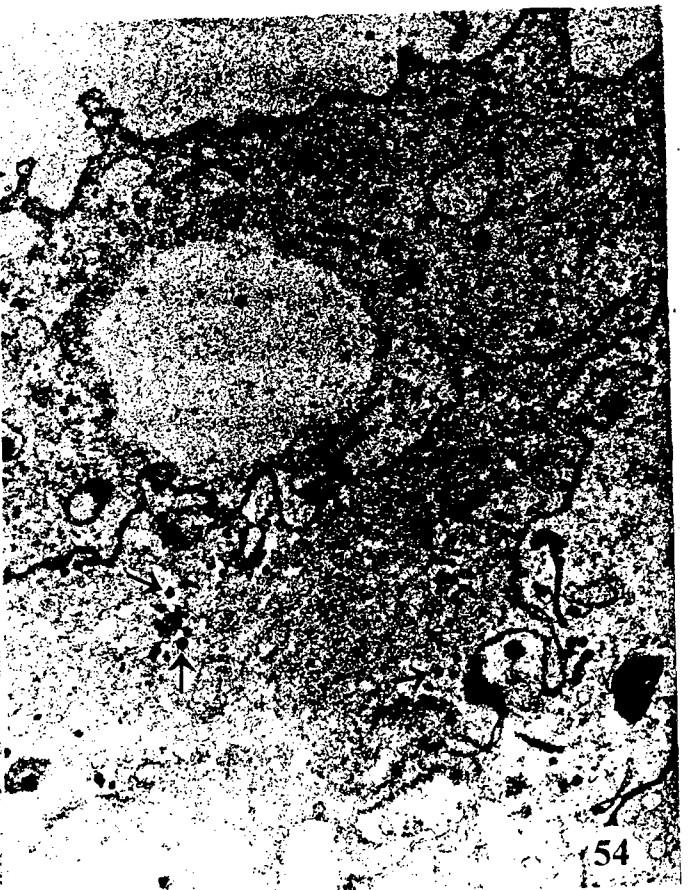

54

55

56

57

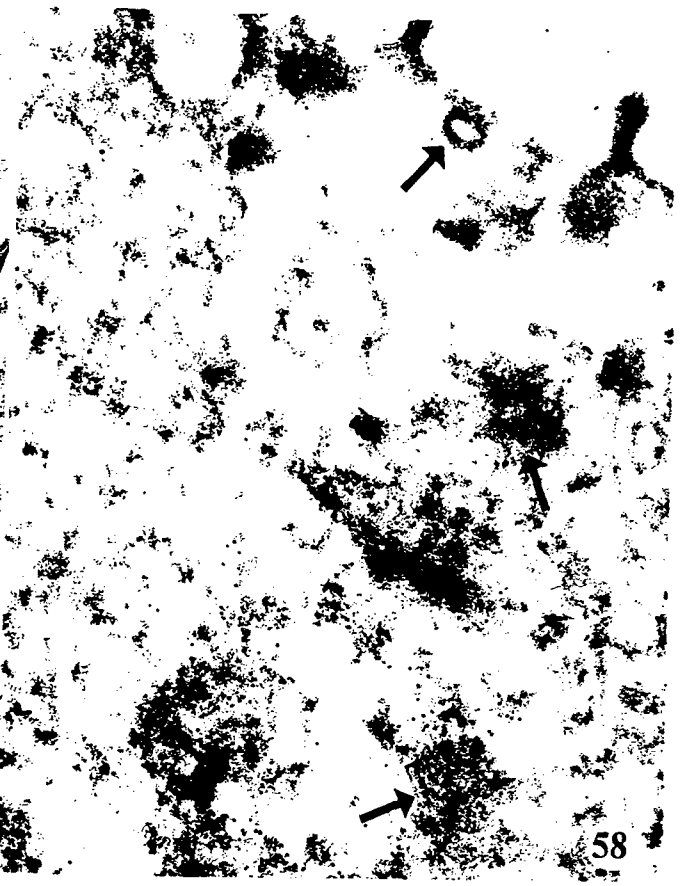

58

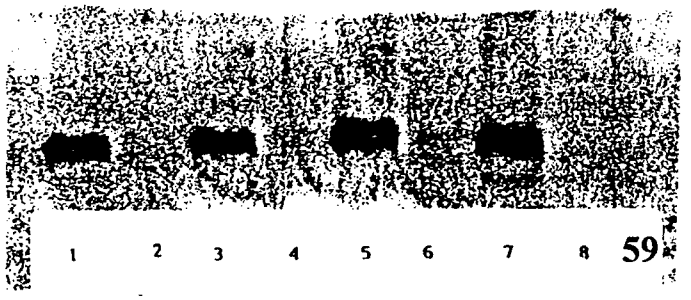
1
2
3
4
5
6
7
8

59

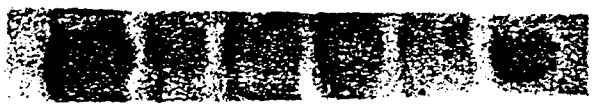
1
2
3
4
5
6

60

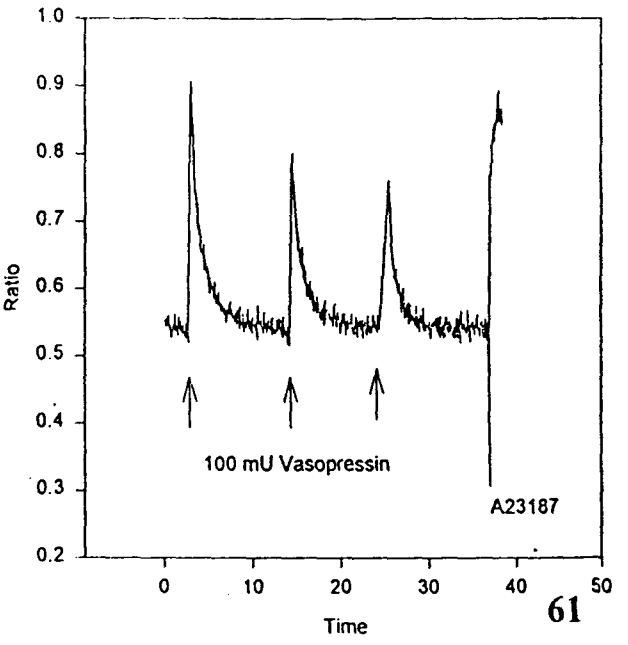
1.0
0.9
0.8
0.7
0.6
0.5
0.4
0.3
0.2
Ratio
100 mU Vasopressin
A23187
0
10
20
30
40
50
Time

61

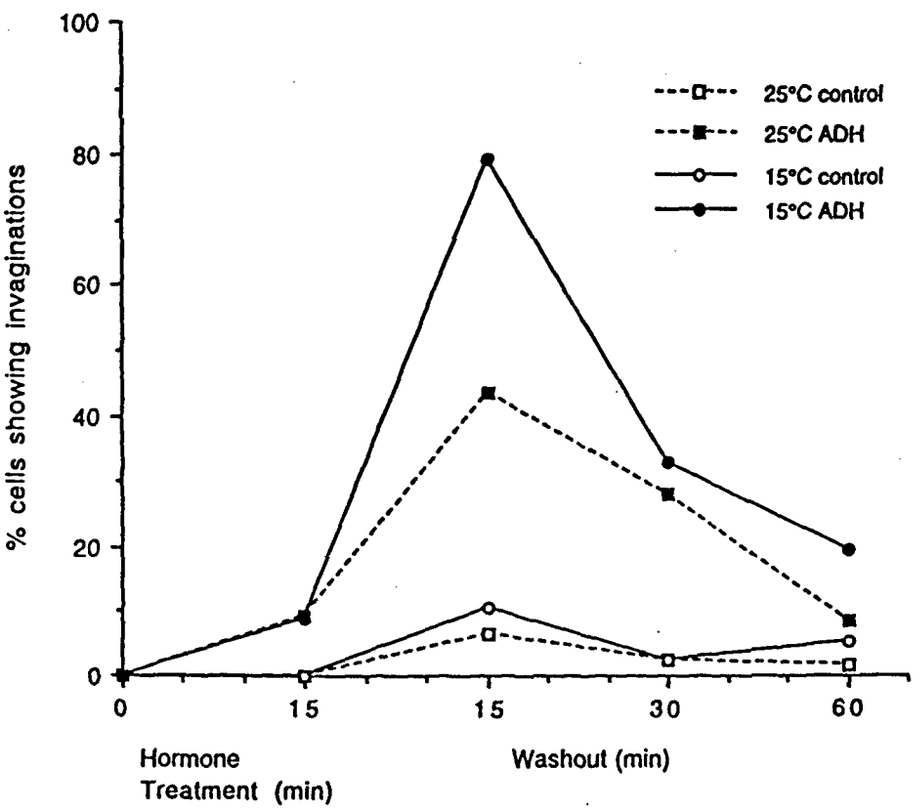

Graph I. Shows the effect of temperature on percent of invaginations at 25° and 15°C in the control and ADH-stimulated TUB sacs at 15 min exocytosis and at 15, 30 and 60 min washout periods.

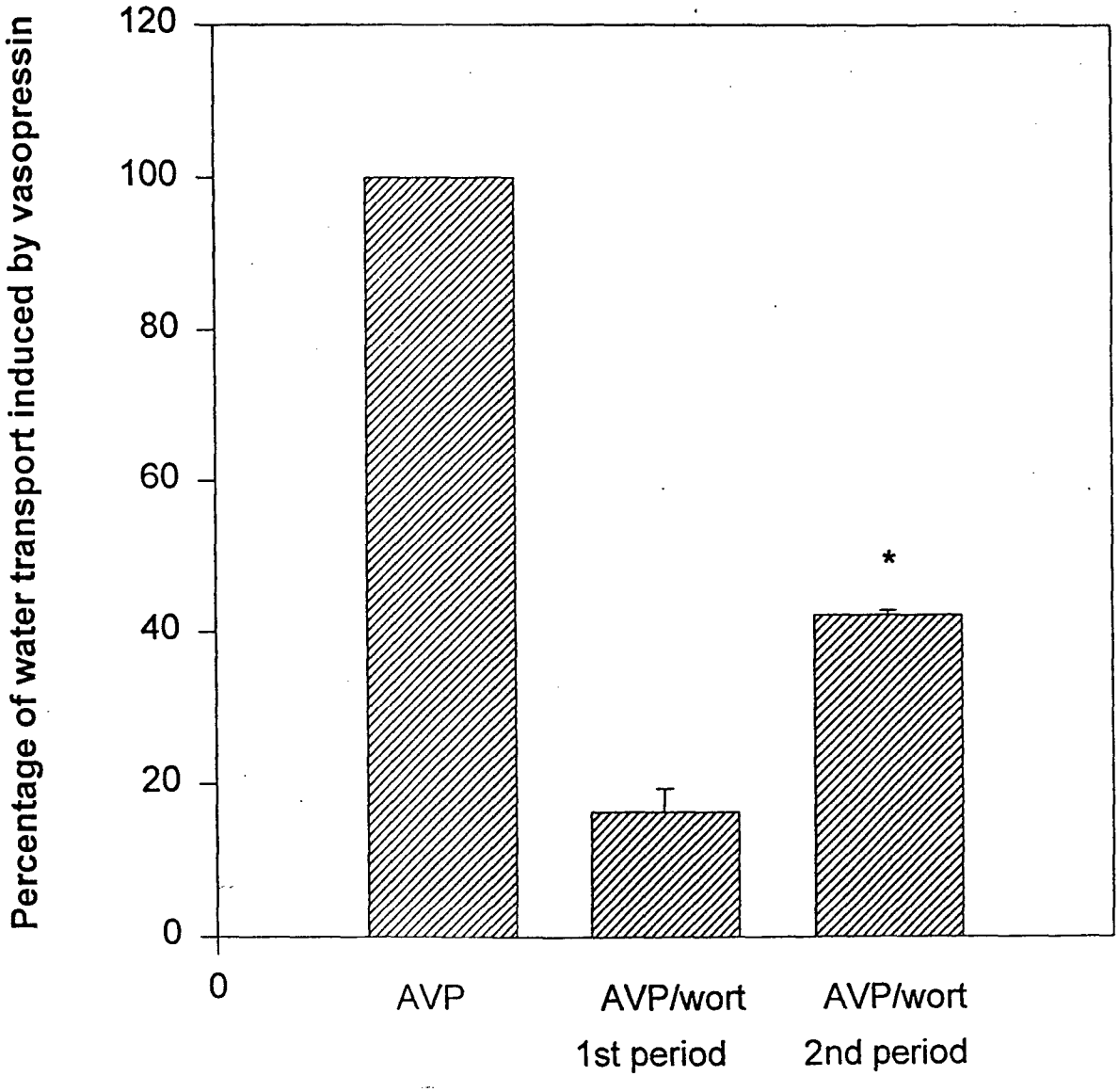
Percentage of water transport induced by vasopressin
120
100
80
60
40
20
0
0
AVP
AVP/wort
1st period
AVP/wort
2nd period
*

Histogram I

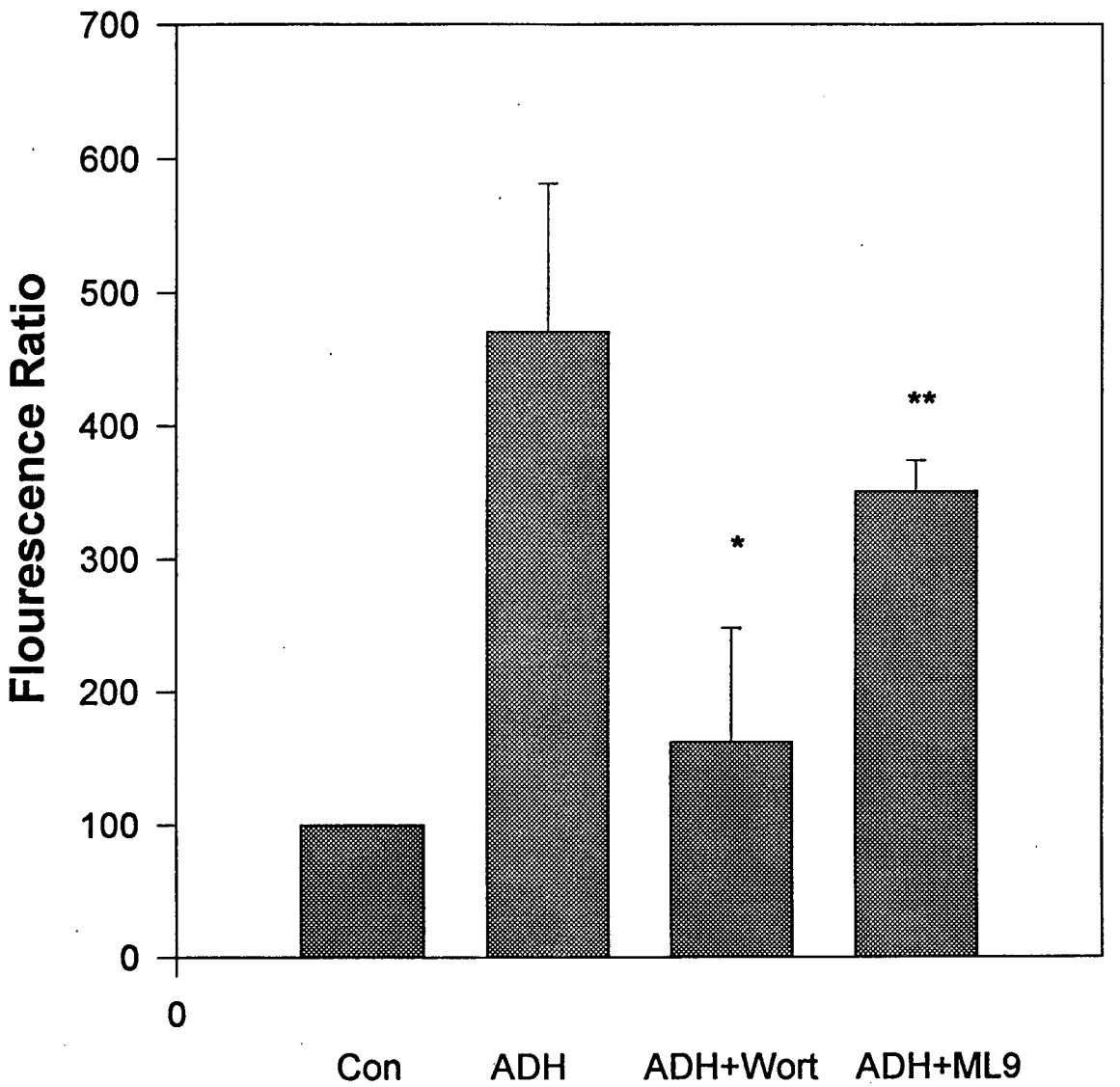

Histogram II